Shale gas potential of Devonian shale in north Yukon: Results from a diamond drillhole study in western Richardson Mountains

Tiffani A. Fraser[1], Tammy L. Allen
Yukon Geological Survey, Whitehorse, YT

Larry S. Lane, Julito C. Reyes
Geological Survey of Canada, Calgary, AB

Fraser, T.A., Allen, T.L., Lane, L.S., and Reyes, J.C., 2012. Shale gas potential of Devonian shale in north Yukon: Results from a diamond drillhole study in western Richardson Mountains. *In:* Yukon Exploration and Geology 2011, K.E. MacFarlane and P.J. Sack (eds.), Yukon Geological Survey, p. 45-74.

ABSTRACT

Fresh diamond drill core samples from Paleozoic shale of the Road River Group and Canol and Imperial formations in the Richardson Mountains, immediately east of Eagle Plain basin, were analysed for Rock-Eval pyrolysis and total organic carbon content, organic petrology, and vitrinite reflectance to assess organic matter quantity, quality, and thermal maturity. X-ray diffraction was conducted to assess quartz, clay, and carbonate mineralogy. Samples are from three areas located along a north-trending strike length of 110 km.

All samples are overmature with respect to oil generation (1.89 to 3.86 $\%Ro_R$). However, values systematically decrease southward along the mountain front through the dry gas window to the upper limit of the mixed wet/dry gas window (2.00 $\%Ro_R$). Organic petrology identified abundant amorphous kerogen with lesser amounts of alginite-derived macerals, and *Tasmanites* alginite in both the Road River Group and Canol Formation while the Imperial Formation was organically lean. Total organic carbon values for the Canol Formation are 0.3 to 20.1 wt % with most samples containing 2 to 5 wt % TOC. For the Road River Group, TOC values are 1.0 to 19.3 wt % with most less than 5 wt %. The Imperial Formation TOC values are mainly below 1 wt %.

X-ray diffraction analyses indicate the succession is highly siliceous, particularly the Canol Formation with quartz values from 91 to 100%. Samples of the Imperial Formation are generally 82 to 90% quartz, while Road River Group samples are more variable with 62 to 96% quartz.

This study suggests that these strata have the potential to host unconventional hydrocarbons in the region under favourable burial conditions. Canol Formation and Road River Group strata have high TOC values and contain identifiable Type I and II organic macerals suggesting they may have been richer source rocks in the past. All strata are highly siliceous and thus good candidates for hydraulic fracture stimulation, with the Canol Formation the most mineralogically consistent of all strata examined.

A 2010 study of subsurface Canol and Imperial formation shale west of the study area indicates these formations are within the oil window, less thermally mature than in the Richardson Mountains. These results highlight the potential for natural gas and liquids in Devonian shale in Eagle Plain basin.

[1] *tiffani.fraser@gov.yk.ca*

INTRODUCTION

In recent years, thick shale deposits have been the target of exploration efforts in many North American basins for their natural gas potential. As thick shale deposits are known to exist in many Yukon sedimentary basins, studies are being made by the Yukon Geological Survey and the Geological Survey of Canada to assess these rocks for their hydrocarbon potential. This paper presents the results of one such study in northern Yukon, immediately east of Eagle Plain basin on the western flank of the Richardson Mountains. The study was made possible by the successful collaboration of geologists from federal and territorial governments, and the minerals and oil and gas sectors.

In 2009, diamond drill core from a 2007-2008 mineral exploration program was retrieved from the field by staff from Northern Cross (Yukon) Limited, the Geological Survey of Canada, and the Yukon Geological Survey. This relatively 'fresh' core was collected for study as it penetrated three Devonian shale formations thought to be prospective for shale gas. Approximately 1500 metres of core was collected from three different localities spanning 110 km, all in the western flank of the Richardson Mountains, immediately east of Eagle Plain basin. Core samples were analysed for thermal maturity, source rock potential, mineralogy, and age. The collection of the core was made possible by donation from Archer, Cathro & Associates (1981) Limited, who conducted exploration activities including diamond drilling in the region on behalf of a third party mineral company.

Preliminary results were previously reported from one of the diamond drill properties, the Rich property, including a 600 m long composite section penetrating the uppermost Road River Group, Canol and lowermost Imperial formations (Allen *et al*., 2011). This paper builds on the previous publication and includes data from two additional properties, Pe to the south and Fox to the north. Analytical work completed on the shale samples highlights the importance of Devonian shale as hosts for unconventional hydrocarbons in northern Yukon.

STUDY AREA

The diamond drill core assessed in this study was retrieved from the Fox, Rich, and Pe properties along the western flank of the southern Richardson Mountains (Fig. 1), immediately east of Eagle Plain basin. The southern Richardson Mountains are north-trending, extending roughly from the Peel River in the south to near where the Dempster Highway crosses the mountain trend adjacent the Northwest Territories/Yukon border (Fig. 1). Eagle Plain basin, an underdeveloped prospective hydrocarbon exploration area in north Yukon, lies between 65.5 and 67.5°N latitudes and 136 and 140°W longitudes (Osadetz *et al*., 2005). North to south, the basin is approximately 170 km long and extends approximately 80 km east to west, covering an area of approximately 20 600 km^2. Tectonic uplift in the region immediately east of the basin exposes Devonian strata where mineral exploration, including diamond drilling, was conducted. The stratigraphic interval, exposed in the range, extends westward across Eagle Plain basin in the subsurface.

The Fox is the northernmost property located on NTS map sheet 116I/16 at 66°56'N latitude and 136°16'W longitude. The property is approximately 70 km northeast of Eagle Plains Hotel which is situated at km 369 of the Dempster Highway (Fig. 1). The Rich property is located on NTS map sheet 116I/08 at latitude 66°19'N and longitude 136°14'W. The property is 23 km southeast of the Eagle Plains Hotel and 65 km south of the Fox property. The Pe is the southernmost property located on NTS map sheets 106E/13 and 116H/16 at latitude 65°56'N and longitude 136°01'W. The property is located approximately 56 km southeast of the Eagle Plains Hotel. The distance between the Rich and Pe properties is approximately 43 km.

GEOLOGICAL SETTING

TECTONIC

Eagle Plain and Richardson Mountains are foreland elements of the Northern Yukon Fold Complex, which sits on the great arc of the Mackenzie Mountains of the northern Cordillera. The complex is a north-striking fold and thrust belt extending 500 km northward from the Ogilvie Mountains to the Beaufort Sea. The deformation that produced the complex culminated in Paleocene-Eocene time (Lane and Dietrich, 1995) in response to regional east-west shortening coeval with the northward-directed deformation that uplifted the Ogilvie Range (Lane, 1998).

The southern Richardson Mountains (Fig. 1) are a faulted anticlinorium that developed by tectonic inversion of the early Paleozoic Richardson trough, either by thick-skinned deformation localized at a felsic-to-mafic basement transition (Lane, 1996) or by thin-skinned deformation transmitted hundreds of kilometres eastward from a distant

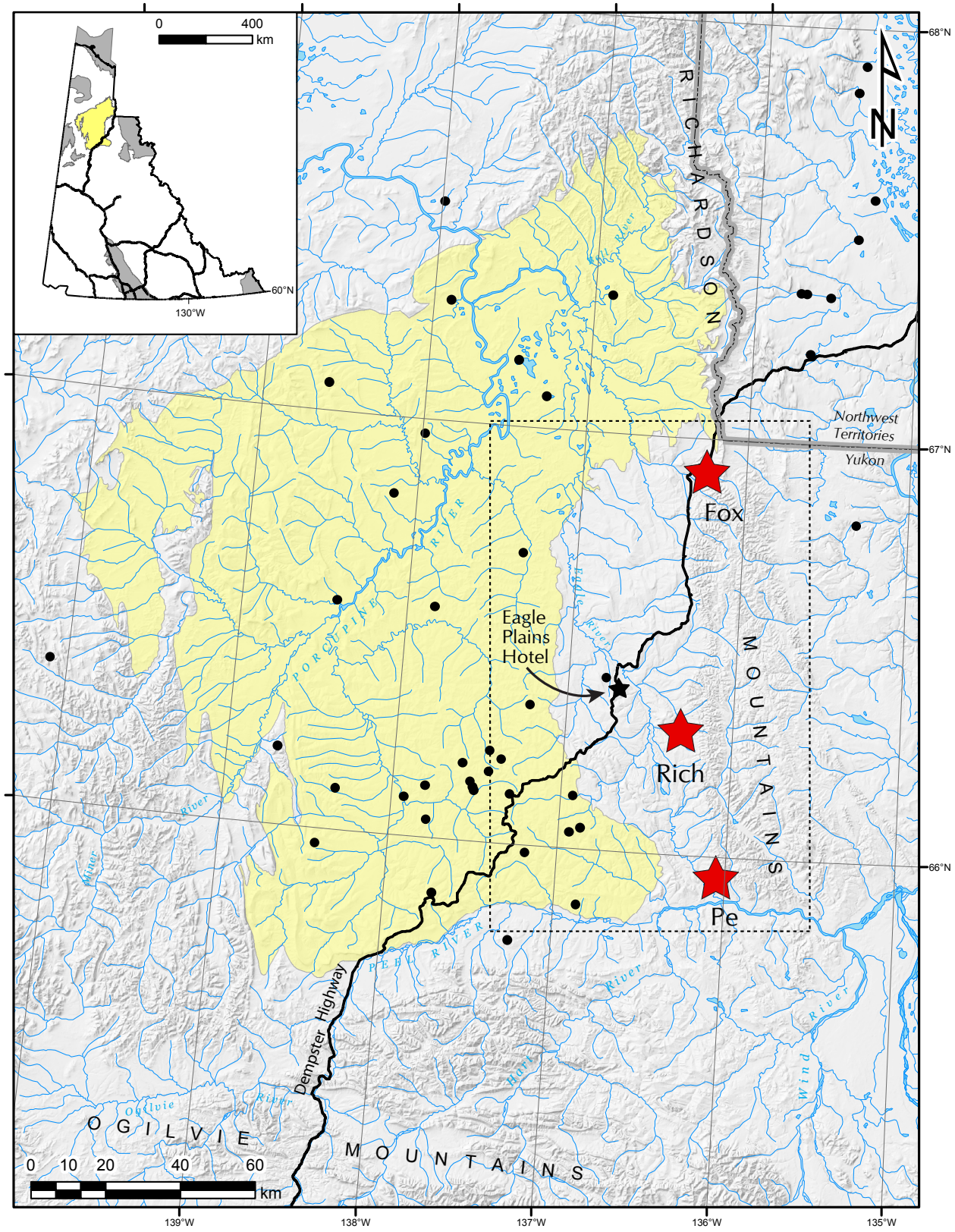

Figure 1. *Map of Eagle Plain basin exploration region (yellow polygon) and the location of the Fox, Rich and Pe properties. Black dots represent oil and gas exploration well locations. Inset map of Yukon with Eagle Plain exploration region in yellow and other oil and gas basins in grey. Dotted box is area displayed in Figure 7.*

hinterland (Hall and Cook, 1998). The eastern part of the anticlinorium has been partially dismembered on sub-vertical faults related to Neogene tectonics (Mazzotti *et al.*, 2008).

The adjacent Eagle Plain basin (Fig. 1) is a mildly deformed foreland-style intermontane basin dominated by gentle north-trending folds that are detached in Proterozoic strata at depth, and are commonly thrust-cored (Lane, 1996; Hall and Cook, 1998), although most of the faults do not project to the surface.

An earlier cycle of deposition and uplift is recorded in the Devonian and Carboniferous successions relevant to this contribution. Widespread carbonate banks on the Northern Interior Platform and Yukon Stable Block, as well as deeper water deposits comprising the Road River Group in the Richardson trough, were drowned abruptly in Middle Devonian time in an event that resulted in the deposition of the Canol Formation over a wide area of northwestern Canada (Morrow, 1999). Soon thereafter an aggregate thickness of several kilometres of turbiditic shale, siltstone, and sandstone of the Imperial and Tuttle formations were deposited through Late Devonian and Early Carboniferous time. These clastic wedge deposits were shed from the Ellesmerian orogen as it encroached into the northern margin of Eagle Plain, resulting in substantial burial (Lane, 2007, 2010). Subsequent uplift and denudation produced a widespread erosional unconformity across Eagle Plain and Peel Plateau that places Early Cretaceous strata directly onto Devonian and Carboniferous rocks in northern and central Eagle Plain; and onto Permian strata in the south.

STRATIGRAPHY

The regional stratigraphic setting is described in Allen *et al.* (2011). Descriptions of Middle Devonian to Carboniferous strata are re-iterated here as they pertain specifically to this study. Of interest is the uppermost Road River Group, Canol and lower Imperial formations. A stratigraphic column for the Silurian to Carboniferous section is shown in Fig. 2, displaying the relationship and ages of the units of interest.

The Road River Group (originally defined by Jackson and Lenz (1962) and elevated to group status by Fritz (1985)) was deposited during Late Cambrian to Middle Devonian time in the Richardson trough and on most of the Yukon Stable Block (Morrow, 1999). In outcrop, the upper portion of this unit is generally a graptolitic, black shale and shaly limestone, although the upper 50 m, and the stratigraphy pertinent to this study, is white weathering, siliceous shale, and chert (Fig. 3). Road River Group strata are thickest in the Richardson trough, at almost 3000 m, however it is thinner on the Yukon Stable Block (Morrow, 1999). Numerous early workers referred to a significant unconformity at the upper contact of the Road River Group with the overlying Canol Formation; more recent workers consider the contact conformable, with the Canol Formation being a condensed section possibly initiated by rapid sea level rise in Givetian time (see discussions in Pugh, 1983 and Morrow, 1999).

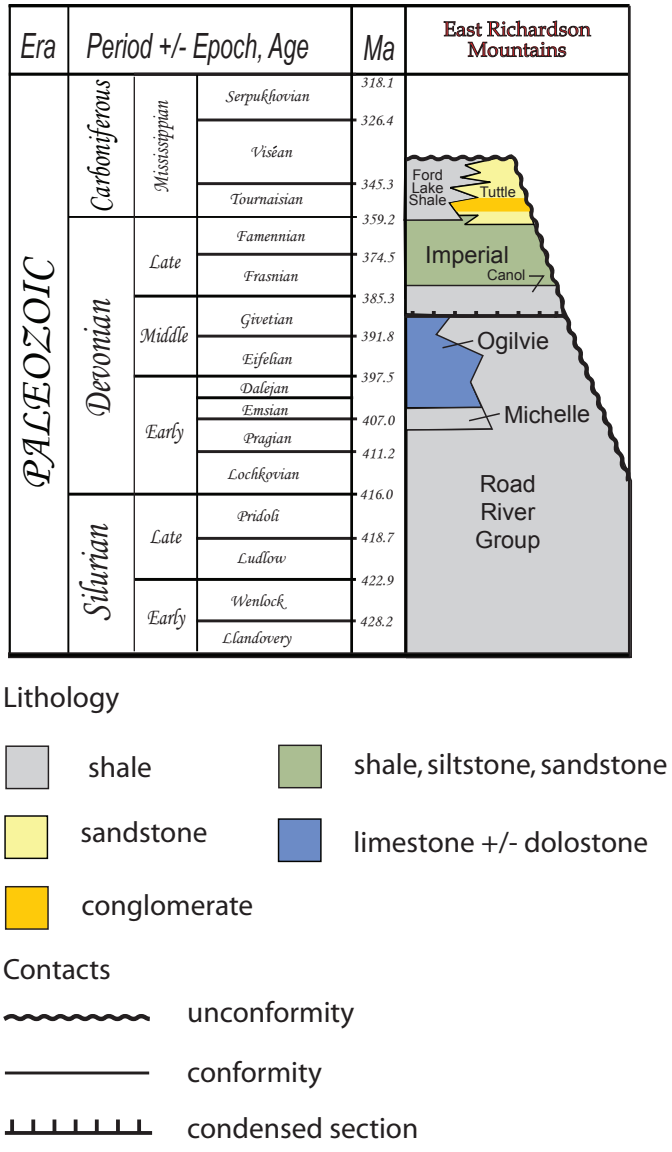

Figure 2. *Stratigraphic column of Silurian to Carboniferous geology of the east Richardson Mountains (modified from Morrow, 1999).*

Figure 3. *Black shale and chert interbedded with resistant, light grey weathered limestone of Road River Group, unnamed creek, NTS map sheet 116I/08.*

The Middle to Upper Devonian (late Givetian and early Frasnian) Canol Formation (Bassett, 1961) is a grey to black, siliceous, thin-bedded, fissile and predominantly non-calcareous shale (Bassett, 1961; Norris, 1985; Fig 4). The Canol Formation is widely distributed over much of Yukon and Northwest Territories. In the Eagle Plain basin it ranges in thickness from approximately 4 to 80 m, based on well intersections (Fraser and Hogue, 2007). It is highly organic and is considered a hydrocarbon source rock for the Norman Wells oil field which has been producing since the 1940s, and continues to be a prominent target for ongoing exploration in that region. In the Richardson Mountains, the Imperial Formation (A.W. Norris, 1997) conformably overlies the Canol Formation.

Figure 4. *Canol Formation as observed on an unnamed creek, NTS map sheet 116I/08. Note the fissile nature of the shale.*

The Upper Devonian Imperial Formation (originally defined by Link, 1921; formalized by Hume and Link, 1945) is a thick package of siliciclastic strata representing shelf, slope, and basin deposits derived from the Ellesmerian orogeny north of the study area (Pugh, 1983; Braman and Hills, 1992). In the western Richardson Mountains, the Imperial Formation consists of three lithologically different units: a lower rusty weathering, siliceous siltstone and shale with minor sandstone (Fig. 5), a middle unit dominated by siliceous siltstone, turbiditic sandstone and shale, and an upper portion of light grey weathering, laminated shale and siltstone with thin orange weathering pyritic sandstone beds. The lower portion has been dated in the study area as Frasnian to Famennian (*e.g.,* Braman and Hills, 1992; Dolby, 2010; Allen *et al.*, 2011). In the subsurface of Eagle Plain, the Imperial Formation attains a maximum thickness of 1229 m in well intersections; and is overlain, depending on location, either conformably by the Ford Lake Shale or Tuttle Formation, or, unconformably by Permian or Cretaceous strata (Fraser and Hogue, 2007; Norris, 1984).

Figure 5. *Imperial Formation strata observed above the Canol Formation on unnamed creek on 116I/08. Note the strata lack fissility and layering that is well established in the Road River Group and Canol Formation. Imperial strata are also lighter in colour.*

PREVIOUS STUDIES

Shale gas research in Yukon is in its infancy, however some published information exists on Upper Devonian shale units in north Yukon. Hamblin (2006), in a report offering a preliminary inventory of shale gas possibilities in Canada, identified Road River Group, Canol and Imperial formation shale units in Eagle Plain as having significant apparent geological potential. That report was compiled solely from existing published data and was meant to

encourage geological studies in certain areas of Canada. Other shale gas literature for Yukon strata includes preliminary results of the research presented in Allen *et al.* (2011) which provided Rock-Eval, mineralogical and palynological determinations of Road River Group, and Canol and Imperial formation strata from Rich property core.

Upper Devonian shale characteristics from field studies in north Yukon have been reported in a number of publications (*e.g.*, Norris, 1985; A.W. Norris, 1997; Richards *et al.*, 1997; Pugh, 1983; Morrow, 1999; Gal *et al., 2009*; Hadlari *et al.*, 2009; Allen, 2010). Rock-Eval/TOC results from Canol and Imperial formation shale (cuttings and/or core) from selected petroleum exploration wells in Eagle Plain basin are reported in Link *et al.* (1989), Snowdon (1988) and Lane *et al.* (2010).

Link *et al.* (1989) used Rock-Eval/TOC and organic petrology to evaluate the petroleum source rock potential of the Phanerozoic succession in northern Yukon and northwestern Northwest Territories (NWT), including Road River Group, Canol and Imperial formation shale. In that study, a substantial set of samples were analysed from outcrop samples collected along the Dempster Highway and from exploration well cuttings throughout the Eagle Plain and Mackenzie Delta region. Also, Link and Bustin (1989) investigated the thermal history and levels of organic maturation of Phanerozoic strata in northern Yukon and northwestern NWT by visual analyses including vitrinite reflectance and conodont alteration index.

Industry exploration for hydrocarbons has been ongoing in Eagle Plain basin from the 1950s to the present. To date, 34 wells have been drilled in the basin to evaluate conventional oil or gas targets, with several discoveries and multiple minor shows from various stratigraphic intervals. This exploration history is summarized in Osadetz *et al.* (2005).

Limited industry exploration for mineral deposits has occurred in the region. A few regional exploration programs targeting lead-zinc mineralization were undertaken in the area during the 1970s with very little of this work filed as assessment reports (Héon, 2006). The reader is directed to Héon (2006) for further details regarding mineral exploration and potential mineral occurrences.

Nickel-rich massive sulphide deposits hosted by Devonian black shale occur in the Richardson Mountains (Goodfellow, 2011). Exploration by Archer, Cathro in 2007 and 2008 resulted in bedrock mapping and a diamond drilling program targeting the strata bound nickel-molybdenum (NiMo) occurrence on the west flank of the Richardson Mountains (Rob Carne, pers. comm., 2010). The occurrence is described as a sheet-like massive sulphide layer enriched with nickel, molybdenum, and zinc located at the contact between the Road River Group and the overlying Canol Formation (Fig. 6). Individual holes penetrated the lowermost Imperial Formation, Canol Formation and uppermost Road River Group; however diamond drilling at the Pe property did not intersect the target (Rob Carne, pers. comm., 2010).

Figure 6. *Contact between the Road River Group and the overlying Canol Formation. The metre-scale iron-stained nodules are commonly observed between the two units. The NiMo zone occurs less than a metre above the nodule horizon. This photo is from an unnamed creek on NTS map sheet 116I/08.*

METHODS

CORE COLLECTION

In September 2009, approximately 1500 m of core was salvaged from the Fox, Rich and Pe properties in order to collect a representative suite of continuous core along the 110 km long north trend of the Canol and Imperial formations. From the Fox property, Road River Group and Canol Formation strata were collected from two drillhole locations (FX07-02 and FX-07-03). From the Rich property, core was collected from six drillhole locations (Rich 07-02, 07-7A, 07-16, 07-20, 08-24 and 08-25) which penetrated either the Imperial or Canol formations or Road River Group strata, or a subset thereof. At the Pe property, Canol Formation core was collected from one drillhole (PE-07-07). The core was slung by helicopter from each mineral property to the Eagle Plains Hotel. From the hotel, the core was transported by truck to the Geological Survey of Canada in Calgary, Alberta. Location information for all core is presented in Figs. 1 and 7 and Table 1.

ANALYTICAL WORK

Analytical work conducted on the shale drill cores includes Rock-Eval pyrolysis and total organic carbon content analysis (RE/TOC) to assess the quantity, quality, type, and thermal maturity of organic matter; vitrinite reflectance (VR) to also assess thermal maturity of organic matter; organic petrology to confirm the type of organic matter; x-ray diffraction (XRD) mineralogy to evaluate rock mineralogy and 'fracability'; and palynological studies to determine stratal age and relationships.

ROCK-EVAL /TOC

Core samples from the Road River Group, Canol and Imperial formations were analysed for organic richness and maturity of organic matter using a Rock-Eval 6 Turbo pyrolysis apparatus in the Organic Geochemistry Laboratory of the Geological Survey of Canada, Calgary. These analyses provide information on organic matter quantity or richness (TOC), quality (OI/HI cross plots), thermal maturity (T_{max}), and ultimately remaining hydrocarbon potential (all parameters combined). RE/TOC samples were selected at a constant spacing measured perpendicular to local bedding, with minor adjustments to ensure suitable lithologies were sampled, and with selective additional sampling near contacts. The core sample spacing was typically every 7-14 m for Fox core, 10-18 m for the Rich core, and typically 10-14 m for the Pe core. A bitumen sample was also included in the sample set.

VITRINITE REFLECTANCE AND ORGANIC PETROLOGY

Vitrinite reflectance (VR) and organic petrology were completed at the Organic Geochemistry Laboratory at GSC Calgary where standard procedures for organic petrology based on Mackowsky (1982) are generally followed. Samples are prepared for incident white and fluorescent light microscopy by crushing them into 1-5 mm particulates, with many also sized to up to 1 cm cubes. The samples were then mounted in an epoxy, ground, and finally polished. Organic petrography was conducted using incident light microscopes equipped with white (halogen; 546 nm) and fluorescent (HBO 100W) light sources, and oil immersion 50X objective. Percent reflectance in oil (%Ro; refractive index of immersion oil = 1.518) was measured with the Leitz MPV II – COMBI system. The number of reflectance measurements made on any given maceral within a sample generally varied from 5 to 50. Random percent reflectance in oil ($\%Ro_R$) was measured (n = 5 to 50) on huminite, primary bitumen, and vitrinite macerals. A Leitz MPM II microscope with a PC-controller system is used for %Ro data collection. Reflectance is calibrated using glass standards (0.506, 1.025, and 1.817 %Ro) of known refractive index.

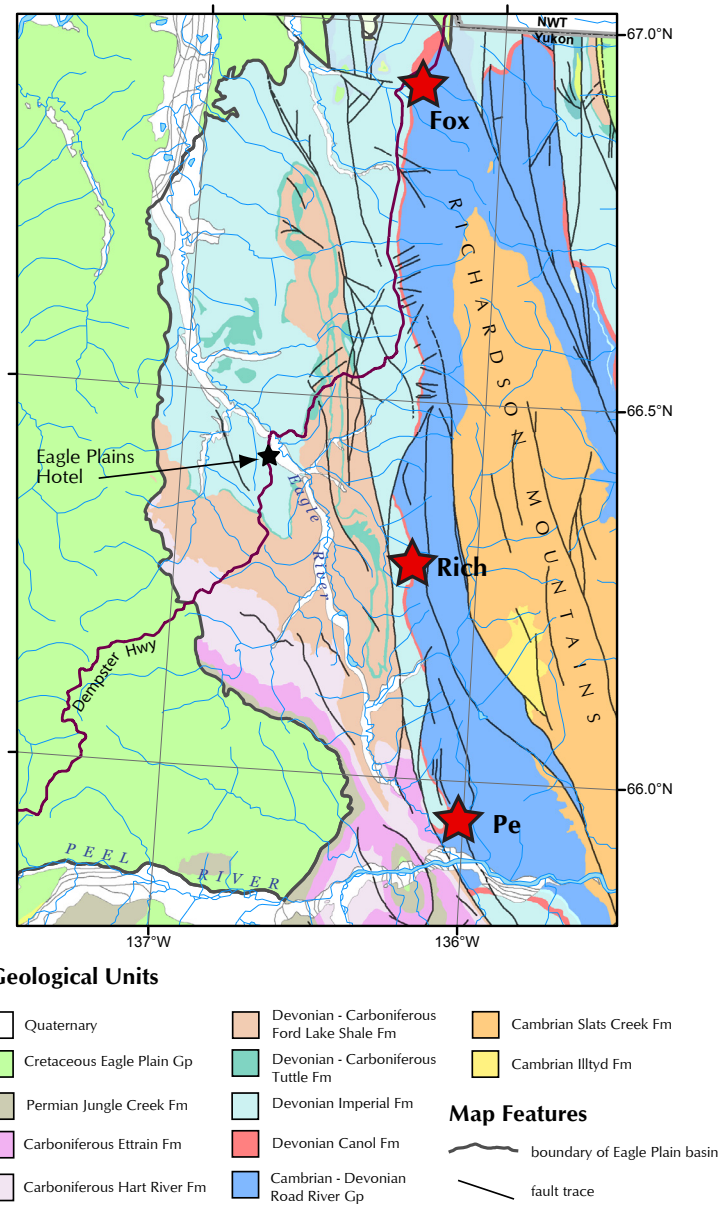

Figure 7. *Geological map showing mineral properties from which diamond drillhole core was retrieved. Geology after Gordey and Makepeace (1999). The location of this map with respect to Eagle Plain basin is displayed in Figure 1.*

Table 1. *Summary of diamond drillholes used in this study. Note that results from the Rich property (excluding vitrinite reflectance) were previously published in Allen et al. (2011). Fx = Fox property, RI = Rich property. The location of the drillhole indicates where the hole was collared.*

Diamond drillhole	Location* (UTM NAD83, Zone 8W)		Unit	Downhole depth		Downhole thickness (m)	Total depth drilled (m)	Core size	Azimuth	Dip
	Easting	Northing		from (m)	to (m)					
FX07-02	442197	7420757					106.68	BTW	110°	-75
			overburden	0	5.92	5.92				
			Imperial Fm	n/a	n/a	0				
			Canol Fm	5.92	68.37	62.45				
			Road River Gp	68.37	106.68	38.31				
FX07-03	442337	7423398					210.31	BTW	110°	-75
			Canol Fm	0	~95.0	~95.0				
			Road River Gp	~95.0	210.31	96.75				
PE07-07	452941	7314197					164.59	BTW	045°	-70
			overburden	0	7.58	7.58				
			Canol Fm	7.58	164.59	157.01				
RI07-02	445508	7353769					176.79	BTW	090°	-50
			overburden	0	24.8	24.8				
			Road River Gp	24.8	176.79	151.99				
RI07-07A	444283	7356805					170.69	BTW	070°	-60
			overburden	0	24.38	24.38				
			Canol Fm	24.38	158.67	134.29				
			Road River Gp	158.67	170.69	12.02				
RI07-16	443054	7359059					121.92	BTW	060°	-75
			overburden	0	16.02	16.02				
			Canol Fm	16.02	91.9	75.88				
			Road River Gp	91.91	121.92	30.01				
RI07-20	444880	7356092					189.28	BTW	060°	-75
			overburden	0	51.3	51.3				
			Canol Fm	51.3	189.28	137.98				
RI08-24	443753	7356495					565.71	HQ and NQ	090°	-70
			overburden	0	8.97	8.97				
			Imperial Fm	8.97	370	361.03				
			Canol Fm	370	565.71	195.71				
RI08-25	444390	7354600					343.50	HQ and NQ	090°	-70
			overburden	0	9.35	9.35				
			Imperial Fm	9.35	343.5	334.15				

*Location refers to where the hole was collared.

Sample spacing for vitrinite reflectance was a minimum of 50 to 60 m, measured perpendicular to bedding. Additional samples were analysed in some instances, particularly close to formational contacts.

XRD MINERALOGY

X-ray diffraction (XRD) is a common method used to determine the mineral composition of shale, which is important in determining a formation's brittleness or 'fracability' (mechanically-induced fracture development). Sampling for semi-quantitative XRD analyses was carried out on shale samples from the Road River Group, Canol and Imperial formations at a typical spacing of 25 m measured perpendicular to bedding, with some additional samples collected in the vicinity of contacts. The XRD analyses were run on a Philips PW1700 powder diffraction system with cobalt x-ray source. All analyses were run on powder mounted samples, and executed by the PANalytical X'Pert Quantify software. Mineral determination was processed by PANalytical's X'pert Highscore program, and the quantification of minerals within samples was calculated from their mineral peak intensities (or peak area). Whole rock results are semi-quantitative and are expressed in mineral ratio percent. Total quartz (including chert), total carbonate, and total clay percentages were summed and recalculated out of 100% based on the XRD analyses, and plotted as ternary diagrams.

ANALYTICAL RESULTS

ROCK-EVAL /TOC

Rock-Eval pyrolysis (RE/TOC) results from drill core samples from the Fox, Rich and Pe properties are summarized in Table 2a. Table 2b summarizes RE/TOC results from Rich property surface field samples. Guidelines for interpreting these data are provided in several publications including Espitalié *et al*. (1985), Peters (1986), Peters *et al.* (2005) and Lafargue *et al*. (1998).

At the Fox property TOC values for Road River Group strata range from 3.7 to 19.3 wt % with the average 10.2 wt %. The 19.3 wt % value is anomalous and by removing this value, the average TOC value lowers to 8.7 wt %. TOC values for the Canol Formation range from 1.5 to 20.1 wt %, with the average 7.5 wt %, and the majority in the 4.6 to 7.6 wt % range. The 20.1 wt % value is anomalous and removing this value results in an average TOC of 6.3 wt % for the Canol at this property.

At the Rich property TOC values for Road River Group strata range from 1.6 to 6.1 wt %, averaging 2.8 wt % with the majority between 1 and 3 wt %. TOC values for Canol Formation strata range from 0.3 to 7.3 wt %, averaging 3.3 wt % with the majority in the 2 to 5 wt % range. TOC values for Imperial Formation strata range from 0.7 to 3.1 wt % with almost 90% of samples containing less than 1 wt % TOC. All TOC contents obtained from outcrop samples collected on the Rich property for the Road River Group and the Canol Formation are within the above mentioned ranges obtained from the diamond drill core samples. The samples of the Imperial Formation from outcrop, range from 0.9 to 5.7 wt % or slightly higher than those from diamond drill core. A TOC value of 5.7 wt % is not typical of the Imperial Formation, however a similar phenomena was documented on Tetlit Creek and Trail River, Yukon where isolated intervals up to 1.65 m thick contained black, organic-rich shale with anomalously high TOC values up to 5.3 wt % (Allen, 2010).

At the Pe property, where only the Canol Formation was intersected, TOC values for all samples range from 1.0 to 5.1 wt %, averaging 2.7 wt % with the majority between 2 and 3 wt %.

Figure 8 summarizes the TOC values by geologic unit. The Road River Group strata range from 1.6 to 19.3 wt %, the Canol Formation ranges from 0.3 to 20.1 wt % with only one sample below 1 wt % and the Imperial Formation ranges from 0.7 to 5.7 wt %, with over 85% of the Imperial samples less than 1 wt %.

All samples in this study have S2 values less than 0.2 mg HC/g rock. When S2 values are this low, the Rock-Eval derived T_{max}, production index (PI) and hydrocarbon index (HI) are often unreliable and should be rejected (Peters, 1986). Low S2 values may be attributed to depletion by oxidation, high thermal maturity, or large amounts of Type IV kerogen present (Peters, 1986). With low S2 values, determination of thermal maturity via Rock-Eval is not possible. Further, determination of kerogen type (*e.g.*, I, II and III) is impossible to deduce from a modified van Krevelen cross plot as the hydrogen indices (HI) are very low. All HI values obtained in this study are below 22 mg HC/g C_{org}, with over 90% of the HI values below 6 mg HC/g C_{org}. With increasing temperature, kerogen loses hydrogen resulting in lower HI values. This results in high maturity samples plotting close to the x-axis of the modified van Krevelen diagram rendering it essentially impossible to determine the evolutionary pathway the samples followed, and therefore impossible to infer the original type of organic matter from Rock-Eval analyses (Fowler *et al.,* 2005).

Table 2a and 2b. *Summary of Rock-Eval/TOC data from diamond drillholes (2a) and outcrop data (2b). Parameters measured and derived from Rock-Eval pyrolysis include TOC = total organic carbon content as percent weight of whole rock; S1 = mg hydrocarbons/g rock; S2 = mg hydrocarbons/g rock; S3 = mg CO_2/g rock; PI = production index (S1/(S1+S2)); HI = hydrogen index ((S2/TOC)x100); OI = oxygen index ((S3/TOC)x100); T_{max} = maximum temperature (°C) at top of S2 peak. Note where S2 values are less than 0.2 mg HC/g rock, the PI and Tmax values are unreliable and should be rejected (Peters, 1986). Vitrinite reflectance (%Ro_R) values obtained from this study are included for reference. Unit RR=Road River Group. Highlighted sample is bitumen.*

Table 2a.

Sample	GSC Curation #	Downhole Depth (m)	Unit	S1	S2	PI	S3	Tmax	TOC	HI	OI	%Ro_R
FX07-02-9	C-491544	18.0	Canol	0.01	0.03	0.22	0.40	611	4.60	1	9	
FX07-02-8	C-491543	25.8	Canol	0.01	0.01	0.62	1.75	343	1.54	1	114	
FX07-02-7	C-491542	40.2	Canol	0.01	0.02	0.27	0.75	611	6.11	0	12	
FX07-02-6	C-491541	52.7	Canol	0.00	0.01	0.37	0.57	291	6.86	0	8	3.24
FX07-02-5	C-491540	57.2	Canol	0.00	0.00	0.76	0.44	611	7.56	0	6	
FX07-02-4	C-491539	64.0	Canol	0.00	0.01	0.33	0.59	610	4.89	0	12	3.41
FX07-02-3	C-491538	79.0	RR	0.01	0.04	0.18	0.12	413	8.23	0	1	3.60
FX07-02-2	C-491537	92.2	RR	0.01	0.01	0.29	0.14	453	3.71	0	4	
FX07-02-1	C-491536	106.7	RR	0.01	0.03	0.27	0.23	611	19.29	0	1	3.85
FX07-03-9	C-491553	33.3	Canol	0.01	0.01	0.44	0.62	611	7.26	0	9	3.59
FX07-03-8	C-491552	47.2	Canol	0.01	0.01	0.41	0.34	611	7.51	0	5	
FX07-03-7	C-491551	60.7	Canol	0.01	0.03	0.24	0.18	394	11.95	0	2	
FX07-03-6	C-491550	74.0	Canol	0.01	0.07	0.17	0.36	396	20.08	0	2	
FX07-03-5	C-491549	87.5	Canol	0.00	0.01	0.28	0.23	423	4.66	0	5	3.87
FX07-03-4	C-491548	100.0	RR	0.00	0.02	0.18	0.12	611	9.08	0	1	
FX07-03-3	C-491547	111.5	RR	0.01	0.03	0.22	0.14	435	7.57	0	2	3.85
FX07-03-2	C-491546	128.6	RR	0.01	0.01	0.45	0.28	611	13.33	0	2	3.86
FX07-03-1	C-491545	139.0	RR	0.01	0.02	0.46	0.26	408	10.31	0	3	3.87
R107-02-6	C-491566	34.0	RR	0.02	0.08	0.19	0.43	607	2.27	4	19	
R107-02-5	C-491565	44.7	RR	0.02	0.08	0.19	0.78	606	2.53	3	31	2.21
R107-02-4	C-491564	58.7	RR	0.02	0.12	0.15	0.21	534	3.43	3	6	
R107-02-3	C-491563	75.8	RR	0.02	0.10	0.16	0.35	343	2.68	4	13	
R107-02-2	C-491562	90.0	RR	0.01	0.07	0.17	0.24	428	2.40	3	10	
R107-02-1	C-491561	105.6	RR	0.01	0.10	0.10	0.24	608	6.06	2	4	2.25
R107-07A-12	C-491526	37.8	Canol	0.01	0.02	0.26	0.18	389	5.12	0	4	2.00
R107-07A-11	C-491525	50.6	Canol	0.01	0.03	0.19	0.13	421	3.66	1	4	
R107-07A-10	C-491524	63.2	Canol	0.00	0.02	0.19	0.10	513	5.65	0	2	
R107-07A-7	C-491521	78.1	Canol	0.01	0.02	0.20	0.15	340	4.71	0	3	
R107-07A-6	C-491520	91.0	Canol	0.00	0.02	0.20	0.09	611	3.61	1	2	2.11
R107-07A-5	C-491519	102.3	Canol	0.00	0.01	0.26	0.07	343	2.42	0	3	2.18
R107-07A-4	C-491518	114.8	Canol	0.01	0.03	0.21	0.07	357	2.43	1	3	
R107-07A-3	C-491517	127.5	Canol	0.01	0.04	0.23	0.09	611	3.60	1	3	
R107-07A-2	C-491516	140.2	Canol	0.01	0.05	0.12	0.08	610	3.73	1	2	2.48
R107-07A-1	C-491515	166.5	RR	0.01	0.02	0.25	0.10	316	2.44	1	4	2.77
R107-16-7	C-491560	25.5	Canol	0.01	**0.04**	0.20	0.09	**522**	**2.11**	2	4	

Table 2a continued.

Sample	GSC Curation #	Downhole Depth (m)	Unit	S1	S2	PI	S3	Tmax	TOC	HI	OI	%Ro_R
R107-16-6	C-491559	42.0	Canol	0.01	**0.05**	0.19	0.13	**606**	**3.76**	1	3	
R107-16-5	C-491558	58.5	Canol	0.01	**0.04**	0.20	0.13	**607**	**4.83**	1	3	2.27
R107-16-4	C-491557	72.9	Canol	0.01	**0.05**	0.16	0.10	**606**	**3.51**	1	3	
R107-16-3	C-491556	86.0	Canol	0.01	**0.02**	0.29	0.11	**606**	**2.53**	1	4	2.43
R107-16-2	C-491555	103.1	RR	0.02	**0.03**	0.32	0.17	**607**	**1.60**	2	11	2.56
R107-16-1	C-491554	121.9	RR	0.01	**0.04**	0.19	0.14	**607**	**1.57**	3	9	2.43
R107-20-7	C-491573	85.9	Canol	0.00	**0.02**	0.16	0.12	**489**	**2.40**	1	5	
R107-20-6	C-491572	102.6	Canol	0.01	**0.03**	0.18	0.20	**607**	**3.60**	1	6	
R107-20-5	C-491571	119.3	Canol	0.01	**0.04**	0.14	0.11	**607**	**3.72**	1	3	2.33
R107-20-4	C-491570	135.9	Canol	0.02	**0.11**	0.13	0.24	**606**	**3.32**	3	7	
R107-20-3	C-491569	152.6	Canol	0.04	**0.10**	0.29	0.30	**607**	**3.64**	3	8	
R107-20-2	C-491568	169.3	Canol?	0.02	**0.08**	0.23	0.21	**606**	**1.74**	5	12	
R107-20-1	C-491567	185.9	Canol?	0.02	**0.07**	0.21	0.23	**604**	**2.92**	2	8	2.51
R108-24-47	C-491514	39.3	Imperial	0.00	**0.01**	0.15	0.11	**609**	**0.73**	1	15	
R108-24-46	C-491513	52.0	Imperial	0.00	**0.02**	0.15	0.03	**610**	**0.66**	3	5	
R108-24-45	C-491512	66.9	Imperial	0.00	**0.03**	0.13	0.00	**609**	**0.79**	4	0	2.33
R108-24-44	C-491511	86.2	Imperial	0.01	**0.04**	0.17	0.00	**601**	**1.21**	3	0	
R108-24-43	C-491510	96.3	Imperial	0.00	**0.03**	0.14	0.05	**609**	**0.82**	4	6	
R108-24-42	C-491509	111.4	Imperial	0.01	**0.05**	0.22	0.05	**334**	**0.87**	6	6	
R108-24-41	C-491508	129.6	Imperial	0.01	**0.18**	0.04	0.10	**436**	**0.81**	22	12	3.00
R108-24-40	C-491507	141.5	Imperial	0.01	**0.03**	0.15	0.01	**607**	**0.79**	4	1	
R108-24-39	C-491506	155.0	Imperial	0.00	**0.02**	0.11	0.09	**609**	**0.77**	3	12	
R108-24-38	C-491505	170.5	Imperial	0.00	**0.03**	0.10	0.06	**608**	**0.79**	4	8	
R108-24-37	C-491504	184.5	Imperial	0.01	**0.04**	0.12	0.33	**609**	**0.83**	5	40	2.68
R108-24-36	C-491503	199.0	Imperial	0.01	**0.03**	0.17	0.18	**385**	**3.09**	1	6	
R108-24-34	C-491501	214.3	Imperial	0.00	**0.03**	0.12	0.04	**609**	**0.76**	4	5	
R108-24-33	C-486500	230.0	Imperial	0.00	**0.03**	0.11	0.06	**609**	**0.85**	4	7	
R108-24-31	C-486498	236.2	Imperial	0.09	**3.04**	0.03	0.94	**608**	**97.96**	3	1	
R108-24-30	C-486497	244.1	Imperial	0.00	**0.02**	0.10	0.07	**605**	**0.88**	2	8	3.11
R108-24-29	C-486496	258.9	Imperial	0.01	**0.06**	0.10	0.21	**499**	**0.73**	8	29	
R108-24-28	C-486495	273.2	Imperial	0.00	**0.02**	0.10	0.06	**607**	**0.79**	3	8	
R108-24-27	C-486494	287.3	Imperial	0.00	**0.03**	0.11	0.00	**607**	**0.76**	4	0	
R108-24-26	C-486493	302.8	Imperial	0.01	**0.03**	0.13	0.09	**609**	**0.89**	3	10	2.89
R108-24-24	C-486491	316.0	Imperial	0.00	**0.03**	0.09	0.12	**608**	**0.94**	3	13	
R108-24-23	C-486490	330.9	Imperial	0.00	**0.03**	0.10	0.09	**609**	**0.91**	3	10	
R108-24-22	C-486489	345.7	Imperial	0.00	**0.03**	0.12	0.01	**359**	**0.83**	4	1	
R108-24-21	C-486488	360.0	Imperial	0.00	**0.03**	0.10	0.34	**568**	**0.72**	4	47	3.09
R108-24-20	C-486487	366.8	Imperial?	0.01	**0.03**	0.13	0.00	**537**	**1.12**	3	0	2.90
R108-24-19	C-486486	376.2	Canol	0.01	**0.04**	0.15	0.11	**608**	**2.69**	1	4	2.90
R108-24-18	C-486485	384.3	Canol	0.00	**0.02**	0.15	0.21	**609**	**3.70**	1	6	2.89
R108-24-17	C-486484	393.0	Canol	0.01	**0.03**	0.16	0.06	**610**	**3.42**	1	2	
R108-24-16	C-486483	401.7	Canol	0.01	**0.03**	0.17	0.25	**609**	**6.45**	0	4	2.77
R108-24-15	C-486482	408.8	Canol	0.01	**0.04**	0.13	0.11	**394**	**2.61**	2	4	

Table 2a continued.

Sample	GSC Curation #	Downhole Depth (m)	Unit	S1	S2	PI	S3	Tmax	TOC	HI	OI	%Ro_R
R108-24-14	C-486481	425.0	Canol	0.01	**0.03**	0.15	0.00	**606**	**2.76**	1	0	2.83
R108-24-13	C-486480	441.0	Canol	0.01	**0.05**	0.12	0.00	**446**	**3.42**	1	0	
R108-24-12	C-486479	458.8	Canol	0.00	**0.02**	0.10	0.00	**609**	**3.08**	1	0	
R108-24-10	C-486476	477.5	Canol	0.01	**0.03**	0.17	0.04	**357**	**2.81**	1	1	
R108-24-9	C-486475	483.3	Canol	0.00	**0.04**	0.08	0.15	**609**	**0.31**	13	48	
R108-24-8	C-486474	494.5	Canol	0.00	**0.00**	0.28	0.17	**541**	**5.01**	0	3	2.76
R108-24-7	C-486473	507.7	Canol	0.01	**0.03**	0.16	0.06	**386**	**4.17**	1	1	
R108-24-6	C-486472	511.7	Canol	0.01	**0.04**	0.17	0.49	**383**	**3.69**	1	13	
R108-24-5	C-486471	521.3	Canol	0.01	**0.04**	0.16	0.27	**371**	**4.61**	1	6	
R108-24-4	C-486470	531.3	Canol	0.01	**0.02**	0.17	0.11	**608**	**7.31**	0	2	
R108-24-3	C-486469	546.5	Canol	0.01	**0.06**	0.13	0.47	**606**	**2.69**	2	17	
R108-24-1	C-486467	565.0	Canol	0.01	**0.03**	0.17	0.04	**420**	**1.64**	2	2	2.88
R108-25-22	C-491595	49.5	Imperial	0.01	**0.03**	0.30	0.06	**607**	**0.67**	4	9	2.09
R108-25-21	C-491594	63.5	Imperial	0.01	**0.02**	0.23	0.08	**606**	**0.60**	3	13	
R108-25-20	C-491593	77.5	Imperial	0.01	**0.02**	0.43	0.16	**607**	**0.57**	4	28	
R108-25-19	C-491592	91.5	Imperial	0.06	**0.09**	0.41	0.14	**271**	**0.72**	12	19	
R108-25-18	C-491591	105.5	Imperial	0.11	**0.08**	0.59	0.10	**334**	**0.71**	11	14	2.08
R108-25-17	C-491590	120.5	Imperial	0.01	**0.05**	0.21	0.11	**605**	**0.75**	7	15	
R108-25-16	C-491589	134.5	Imperial	0.02	**0.03**	0.37	0.11	**473**	**0.74**	4	15	
R108-25-15	C-491588	148.5	Imperial	0.01	**0.06**	0.15	0.16	**607**	**0.74**	8	22	
R108-25-14	C-491587	163.8	Imperial	0.01	**0.03**	0.14	0.06	**607**	**0.76**	4	8	2.25
R108-25-13	C-491586	179.1	Imperial	0.01	**0.04**	0.23	0.12	**434**	**0.76**	5	16	
R108-25-12	C-491585	194.4	Imperial	0.01	**0.04**	0.17	0.08	**606**	**2.16**	2	4	
R108-25-11	C-491584	209.7	Imperial	0.01	**0.02**	0.27	0.09	**607**	**0.76**	3	12	
R108-25-10	C-491583	225.1	Imperial	0.01	**0.03**	0.25	0.14	**422**	**0.85**	4	16	2.41
R108-25-9	C-491582	240.4	Imperial	0.02	**0.04**	0.35	0.09	**605**	**0.78**	5	12	
R108-25-8	C-491581	255.7	Imperial	0.01	**0.04**	0.26	0.07	**605**	**0.71**	6	10	
R108-25-7	C-491580	271.0	Imperial	0.01	**0.05**	0.21	0.11	**607**	**2.13**	2	5	
R108-25-5	C-491578	286.5	Imperial	0.02	**0.04**	0.33	0.08	**607**	**0.80**	5	10	2.32
R108-25-4	C-491577	300.6	Imperial	0.01	**0.03**	0.26	0.08	**607**	**0.90**	3	9	
R108-25-3	C-491576	314.7	Imperial	0.01	**0.04**	0.15	0.06	**606**	**0.71**	6	8	
R108-25-2	C-491575	329.1	Imperial	0.02	**0.04**	0.35	0.10	**292**	**0.82**	5	12	
R108-25-1	C-491574	343.5	Imperial	0.01	**0.04**	0.23	0.09	**605**	**0.76**	5	12	2.47
PE07-07-9	C-491535	67.6	Canol	0.01	**0.10**	0.10	0.48	**605**	**2.52**	4	19	
PE07-07-8	C-491534	82.5	Canol	0.01	**0.03**	0.26	0.08	**609**	**2.15**	1	4	
PE07-07-7	C-491533	96.0	Canol	0.01	**0.04**	0.12	0.07	**489**	**2.60**	2	3	
PE07-07-6	C-491532	99.4	Canol	0.01	**0.05**	0.15	0.31	**499**	**5.12**	1	6	1.89
PE07-07-5	C-491531	109.7	Canol	0.01	**0.10**	0.11	0.09	**608**	**2.83**	4	3	1.97
PE07-07-4	C-491530	123.4	Canol	0.01	**0.04**	0.18	0.07	**593**	**1.00**	4	7	
PE07-07-3	C-491529	137.2	Canol	0.01	**0.03**	0.32	0.15	**609**	**1.20**	2	13	
PE07-07-2	C-491528	151.4	Canol	0.01	**0.07**	0.16	0.13	**485**	**4.47**	2	3	
PE07-07-1	C-491527	164.2	Canol	0.01	**0.06**	0.18	0.07	**606**	**2.55**	2	3	1.82

Table 2b.

Sample	GSC curation #	Unit	NAD 83 Zone 8 Easting	Northing	S1	S2	PI	S3	T_{max}	TOC	HI	OI
10TLA-RICH-09P		Imperial	443605	7357239	0.00	0.03	0.14	0.25	609	0.87	3	29
10TLA-RICH-09O		Imperial	443605	7357239	0.01	0.04	0.24	0.37	479	5.68	1	7
10TLA-RICH-09N		Imperial	443865	7357101	0.00	0.03	0.10	0.47	609	1.02	3	46
10TLA-RICH-09M	C-542085	Canol	443994	7357127	0.01	0.04	0.17	0.72	482	2.94	1	24
10TLA-RICH-09K	C-542084	Canol	444442	7357098	0.01	0.03	0.20	0.34	352	3.12	1	11
10TLA-RICH-09I	C-542083	RR	444611	7356939	0.01	0.03	0.16	0.26	610	2.65	1	10
10TLA-RICH-09G		RR	444927	7356821	0.00	0.05	0.08	1.01	609	4.96	1	20
10TLA-RICH-09F		RR	444944	7356815	0.01	0.04	0.12	2.14	609	4.66	1	46
10TLA-RICH-09D		RR	444967	7356804	0.01	0.04	0.15	1.04	609	2.42	2	43
10TLA-RICH-09B		RR	445304	7356761	0.01	0.03	0.15	0.58	610	1.02	3	57
10TLA-RICH-09A		RR	445902	7356439	0.01	0.08	0.07	1.71	522	3.22	2	53

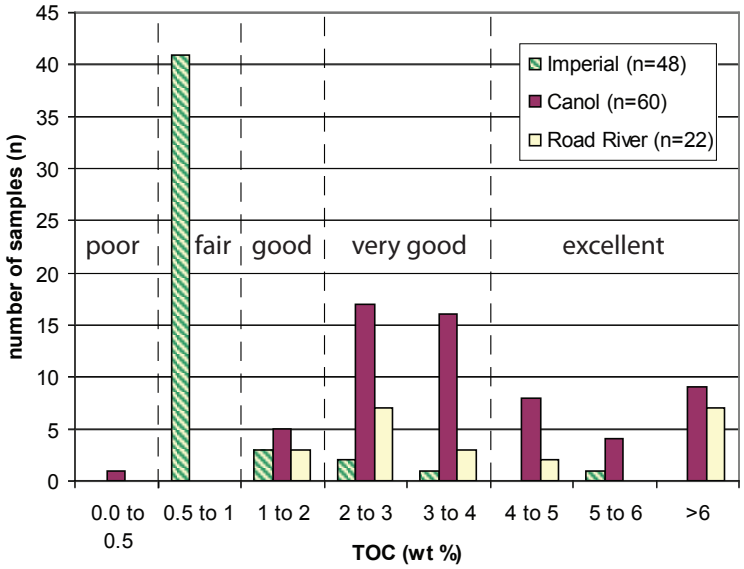

Figure 8. *Histogram summarizing the total organic carbon (TOC) content, expressed in weight percent (wt %), from samples of Road River Group, Canol and Imperial formations from both drill core and outcrop samples. The TOC categories (good to excellent) correspond to source rock generative potential (Peters et al., 2005). See Table 2 for corresponding dataset.*

VITRINITE REFLECTANCE AND ORGANIC PETROLOGY

In order to determine thermal maturity, vitrinite reflectance, a widely accepted method by the oil and gas industry (Fowler *et al.*, 2005; Peters *et al.*, 2005), is an especially important technique when the T_{max} values are rendered meaningless. Table 3 summarizes VR data collected from all drillholes. Appendix A is a detailed table which includes vitrinite reflectance values and comments about the organic material observed in each sample based on organic petrology. From shale samples collected at the Fox property, vitrinite reflectance values range from 2.99 to 3.86 $\%Ro_R$ for the Road River Group (n=5) and 2.91 to 3.59 $\%Ro_R$ for the Canol Formation (n=4). At the Rich property, VR data derived from diamond drill core samples of Road River Group strata range from 2.21 to 2.77 $\%Ro_R$ (n=5); for the Canol Formation from 2.07 to 2.90 $\%Ro_R$ (n=14); and for the Imperial Formation from 2.09 to 3.11 $\%Ro_R$ (n=13). VR values for Canol Formation strata at the Pe property range from 1.89 to 1.97 $\%Ro_R$ (n=3). Thermal maturity values from all samples are very high, with all samples from the Fox and the Rich properties in the dry gas zone (>2.00 $\%Ro_R$), and samples from the Pe property (Canol) near the upper limit of the mixed wet/dry gas zone (just below 2.00 $\%Ro_R$; Mukhopadhyay, 1994).

Organic petrology of the Road River Group samples identified mainly amorphous kerogen with rare to trace amounts of alginite derived vitrinite macerals, chitinozoans, radiolarians and *Tasmanites* alginite (refer to Appendix A for more detailed descriptions). The organic-rich black shale of the Canol Formation contains mainly amorphous kerogen, with minor alginite, alginite derived vitrinite and bitumen (pyrobitumen and migra-bitumen) macerals, negligible terrestrial plant derived inertinite macerals, trace *Tasmanites*, chitinozoans and radiolaria. Both the Road River Group and Canol Formation contain framboidal and tetrahedral pyrite. Imperial Formation

Table 3. *Summary of vitrinite reflectance data in random percent reflectance in oil (% Ro_R) from diamond drill holes. Grey cells represent vitrinite equivalent values for measured pyrobitumen macerals based on Jacob (1989). See Appendix A for more detail including descriptions of macerals.*

Sample #	Downhole depth (m)	Unit	$\%Ro_R$
FX07-02-6	52.7	Canol	2.91
FX07-02-4	64.0	Canol	3.00
FX07-02-3	79.0	Road River	3.09
FX07-02-1	106.9	Road River	3.11
FX07-03-9	33.3	Canol	3.59
FX07-03-5	87.5	Canol	3.13
FX07-03-3	111.5	Road River	3.14
FX07-03-2	128.6	Road River	3.86

Table 3 continued.

Sample #	Downhole depth (m)	Unit	$\%Ro_R$
FX07-03-1	139.0	Road River	2.99
RI07-02-5	44.7	Road River	2.21
RI07-02-1	105.6	Road River	2.25
RI07-07A-12	37.8	Canol	2.07
RI07-07A-6	91.0	Canol	2.28
RI07-07A-5	102.3	Canol	2.30
RI07-07A-2	140.2	Canol	2.48
RI07-07A-1	166.5	Road River	2.77
RI07-16-5	58.5	Canol	2.27
RI07-16-3	86.0	Canol	2.43
RI07-16-2	103.1	Road River	2.56
RI07-16-1	121.9	Road River	2.43
RI07-20-5	119.3	Canol	2.33
RI07-20-1	185.9	Canol?	2.51
R108-24-45	66.9	Imperial	2.33
R108-24-41	129.6	Imperial	3.00
R108-24-37	184.5	Imperial	2.68
R108-24-30	244.1	Imperial	3.11
R108-24-26	302.8	Imperial	2.89
R108-24-21	360.0	Imperial	3.09
R108-24-20	366.8	Imperial	2.90
R108-24-19	376.2	Canol	2.90
R108-24-18	384.3	Canol	2.89
R108-24-16	401.7	Canol	2.77
R108-24-14	425.0	Canol	2.83
R108-24-8	494.5	Canol	2.76
R108-24-1	565.0	Canol	2.88
RI08-25-22	49.5	Imperial	2.09
RI08-25-18	105.5	Imperial	2.08
RI08-25-14	163.8	Imperial	2.25
RI08-25-10	225.1	Imperial	2.41
RI08-25-5	286.5	Imperial	2.32
RI08-25-1	343.5	Imperial	2.47
PE07-07-6	99.40	Canol	1.89
PE07-07-5	109.70	Canol	1.97
PE07-07-1	164.20	Canol	1.89

samples are described as organically lean and as containing minor vitrinite and bitumen macerals and some inertinite macerals (see Appendix A for full details).

XRD MINERALOGY

XRD mineralogy ternary diagrams for percentage of quartz, carbonate, and clay for Road River Group and Canol and Imperial formation shale are provided in Figure 9. Table 4 lists the simplified XRD mineralogy data for each sample, re-calculated from raw data to enable plotting on quartz, carbonate, and clay ternary diagrams. Appendix B lists the XRD mineralogy raw data which includes other minerals not included on the ternary diagrams.

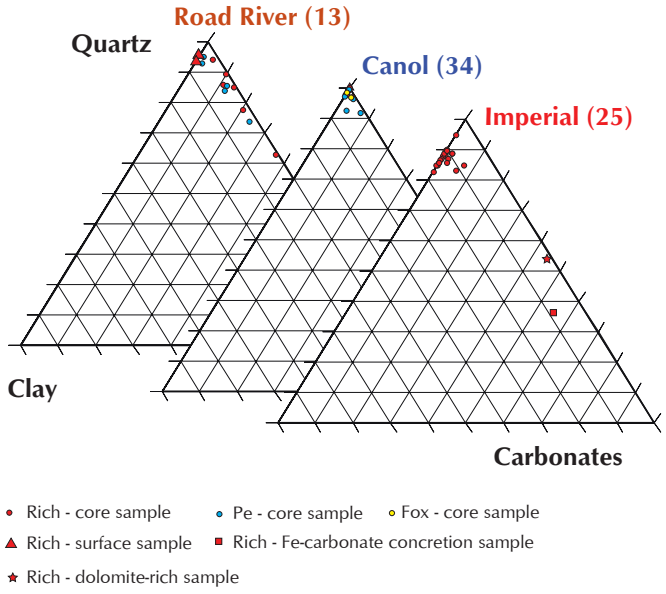

Figure 9. *Ternary diagram displaying the relative mineralogical compositions of Road River Group, Canol and Imperial formation drill core and surface field samples. The corresponding data are in Table 4.*

Road River Group shale samples were analysed from the Rich and Fox properties (n=6 and 5, respectively). In addition, two samples from Road River Group strata exposed at the surface of the Rich property were analysed. Road River shale has the most variable lithology observed, with quartz ranging between 62 and 96%, and carbonate between 0 to 37%. Carbonate is mainly calcite (up to 34%) with minor dolomite (typically ≤2%), except for two samples from the Fox property which had 8 and 11% dolomite. Percentage of clay in all samples was very low, ≤4% mica/illite.

Canol Formation shale was analysed from drill core at the Fox, Rich, and PE properties (n=6, 23, and 4, respectively). In addition, one sample from Canol Formation exposed at the surface of the Rich property was analysed. The Canol Formation, from all properties, is highly siliceous, in all instances exceeding 91% quartz, and typically ≥ 95% quartz. Carbonate and clay fractions are very minor in these samples, typically ≤2% except at the Fox property where higher values of carbonate (up to 7% calcite/dolomite) and up to 4% clay minerals (mica/illite) were found. Of note is one sample from the Fox property which had ~41% gypsum identified.

Twenty-three shale samples from the Imperial Formation were analysed from the Rich property drill core. The Imperial is less siliceous than the Canol Formation but is a more homogeneous lithology than the Road River Group shale sampled from the core. The quartz fraction in all instances of Imperial Formation is >82% with the clay fraction 5 to 17% (chlinochlore, mica/illite, and other mixed layer clays). The carbonate fraction is mainly dolomite (≤2%; n=5) with lesser calcite (2%; n=1), and siderite was found in three samples (≤2%). A number of Imperial samples had minor amounts of Na-feldspar. In addition to the shale samples, two carbonate-rich samples from the Imperial Formation including one dolomite-rich sample (45% total carbonate) and one siderite concretion (55% siderite) are included in Figure 9. Caution should be used with these results as the amount of quartz tends to be overestimated and clay underestimated in many shale samples using standard XRD techniques (Spencer *et al.*, 2010).

DISCUSSION

HYDROCARBON POTENTIAL

Determination of TOC values are used to evaluate source rock generative potential (Peters, 1986). In addition, quantity of TOC is critical in assessing potential shale gas reservoirs as organic matter provides necessary porosity and adsorptive sites for hydrocarbons (Faraj, 2009; Passey *et al.*, 2010). Based on TOC values, the Road River Group and the Canol Formation are organic-rich and demonstrate the most promising prospect as potential source rocks, with predominantly very good to excellent generative potential (Peters, 1986; Fig. 8). Road River Group and Canol Formation strata typically contain 2 to 5 wt % TOC, while the Imperial Formation generally has less than one weight per cent. Because of the high thermal maturity of

Table 4. *Summary of mineral compositions, recalculated from raw data, based on XRD semi-quantitative analysis (expressed in mineral ratio percent) of black shale core samples. Highlighted samples refer to carbonate-rich shale (R108-24-21) and a siderite nodule (R108-24-25). ** = surface samples; NAD83, Zone 8; 10TLA-RICH-09M (443994, 7357127), 10TLA-RICH-09I (444611, 7356939), 10TAL-RICH-09K (444442, 7357098).*

Sample	GSC curation #	Downhole Depth (m)	Formation	% quartz	% carbonate	% clay
RI08-25-22	C-491595	49.5	Imperial	85.4	0.0	14.6
RI08-25-20	C-491593	77.5	Imperial	82.7	6.1	11.2
RI08-25-18	C-491591	105.5	Imperial	89.5	0.0	10.5
RI08-25-16	C-491589	134.5	Imperial	89.7	0.0	10.3
RI08-25-14	C-491587	163.8	Imperial	85.4	2.1	12.5
RI08-25-12	C-491585	194.4	Imperial	88.4	2.1	9.5
RI08-25-10	C-491583	225.1	Imperial	88.7	0.0	11.3
RI08-25-8	C-491581	255.7	Imperial	85.7	0.0	14.3
RI08-25-5	C-491578	286.5	Imperial	86.7	0.0	13.3
RI08-25-3	C-491576	314.7	Imperial	86.5	0.0	13.5
RI08-25-1	C-491574	343.5	Imperial	86.7	0.0	13.3
RI08-24-47	C-491514	39.3	Imperial	89.4	0.0	10.6
RI08-24-45	C-491512	66.9	Imperial	87.5	1.0	11.5
RI08-24-43	C-491510	96.3	Imperial	88.5	2.1	9.4
RI08-24-41	C-491508	129.6	Imperial	84.5	0.0	15.5
RI08-24-39	C-491506	155.0	Imperial	87.8	0.0	12.2
RI08-24-37	C-491504	184.5	Imperial	82.7	0.0	17.3
RI08-24-34	C-491501	214.3	Imperial	88.8	0.0	11.2
RI08-24-30	C-486497	244.1	Imperial	85.7	0.0	14.3
RI08-24-28	C-486495	273.2	Imperial	84.7	0.0	15.3
RI08-24-26	C-486493	302.8	Imperial	86.7	2.0	11.2
RI08-24-25	C-486492	315.2	Imperial	36.0	55.0	9.0
RI08-24-23	C-486490	330.9	Imperial	84.4	7.3	8.3
RI08-24-21	C-486488	360.0	Imperial	52.9	44.7	2.4
RI08-24-20	C-486487	366.8	Imperial?	94.6	0.0	5.4
FX07-02-8	C-491543	25.8	Canol	96.4	0.0	3.6
FX07-02-6	C-491541	52.7	Canol	98.9	0.0	1.1
FX07-02-4	C-491539	64.0	Canol	98.9	0.0	1.1
FX07-03-9	C-491553	33.3	Canol	95.9	3.1	1.0
FX07-03-7	C-491551	60.7	Canol	92.4	3.3	4.3
FX07-03-5	C-491549	87.5	Canol	91.8	7.2	1.0
RI07-07A-12	C-491526	37.8	Canol	98.9	0.0	1.1
RI07-07A-10	C-491524	63.2	Canol	97.8	0.0	2.2
RI07-07A-6	C-491520	91.0	Canol	98.0	1.0	1.0
RI07-07A-5	C-491519	102.3	Canol	98.9	0.0	1.1
RI07-07A-4	C-491518	114.8	Canol	97.9	0.0	2.1
RI07-07A-2	C-491516	140.2	Canol	98.0	1.0	1.0

Table 4 continued.

Sample	GSC curation #	Downhole depth (m)	Formation	% Quartz	% Carbonate	% Clay
RI07-16-7	C-491560	25.5	Canol	97.9	0.0	2.1
RI07-16-5	C-491558	58.5	Canol	97.9	0.0	2.1
RI07-16-3	C-491556	86.0	Canol	99.0	0.0	1.0
RI07-20-7	C-491573	85.9	Canol	99.0	0.0	1.0
RI07-20-5	C-491571	119.3	Canol	99.0	0.0	1.0
RI07-20-3	C-491569	152.6	Canol	98.0	1.0	1.0
RI07-20-1	C-491567	185.9	Canol?	98.0	0.0	2.0
RI08-24-19	C-486486	376.2	Canol	96.9	2.0	1.0
RI08-24-18	C-486485	384.3	Canol	97.9	0.0	2.1
RI08-24-17	C-486484	393.0	Canol	98.0	0.0	2.0
RI08-24-16	C-486483	401.7	Canol	97.8	0.0	2.2
RI08-24-14	C-486481	425.0	Canol	98.9	0.0	1.1
RI08-24-12	C-486479	458.8	Canol	100.0	0.0	0.0
RI08-24-8	C-486474	494.5	Canol	99.0	0.0	1.0
RI08-24-7	C-486473	507.7	Canol	98.9	0.0	1.1
RI08-24-4	C-486470	531.3	Canol	98.9	0.0	1.1
RI08-24-1	C-486467	565.0	Canol	100.0	0.0	0.0
10TLA-RICH-09M**	C-542085		Canol	99.0	0.0	1.0
PE07-07-8	C-491534	82.5	Canol	95.8	3.1	1.0
PE07-07-5	C-491531	109.7	Canol	98.0	0.0	2.0
PE07-07-3	C-491529	137.2	Canol	97.8	0.0	2.2
PE07-07-1	C-491527	164.2	Canol	97.9	0.0	2.1
RI07-07A-1	C-491515	166.5	RR	93.9	4.1	2.0
RI07-16-2	C-491555	103.1	RR	62.2	36.7	1.0
RI07-16-1	C-491554	121.9	RR	88.9	10.1	1.0
RI07-02-5	C-491565	44.7	RR	85.3	11.6	3.2
RI07-02-3	C-491563	75.8	RR	77.3	20.6	2.1
RI07-02-1	C-491561	105.6	RR	84.4	14.6	1.0
10TLA-RICH-09I**	C-542083		RR	94.9	0.0	5.1
10TLA-RICH-09K**	C-542084		RR	93.8	0.0	6.2
FX07-02-3	C-491538	79.0	RR	95.7	1.1	3.3
FX07-02-1	C-491536	106.7	RR	93.7	2.1	4.2
FX07-03-3	C-491547	111.5	RR	84.2	12.6	3.2
FX07-03-2	C-491546	128.6	RR	73.2	24.7	2.1
FX07-03-1	C-491545	139.0	RR	85.7	13.3	1.0

these samples (≥1.89 %Ro_R), care should be taken when using TOC values to describe source rock potential. First, as a source rock matures, the amount of organic matter in the source rock will decrease as hydrocarbons are created, resulting in a decrease in TOC values as the amount of reactive kerogen gets consumed (Daly and Edman, 1987). Tissot and Welte (1984) suggest that for Type II organic matter, hydrocarbon utilizes roughly half of the initial TOC. Using this rule of thumb, and recognizing that the original type of organic matter in the samples may have been variable, the initial TOC of the samples could have been higher, for example in the 4-10 wt % range for the Canol Formation and Road River Group, and between 1 and 2 wt % for the Imperial Formation. Second, TOC by itself is not necessarily a good indicator of how much hydrocarbon a rock can generate (Dembicki, 2009). For organic matter to generate hydrocarbons, the carbon must have associated hydrogen. An indirect measure of hydrogen is the Rock-Eval derived S2 value which is a quantification of the hydrocarbons formed during the thermal decomposition of the kerogen in the rock (Dembicki, 2009). In this study, all strata have Rock-Eval S2 values below 0.2 mg HC/g rock, indicating that there is almost no hydrogen available for generating hydrocarbons, suggesting the source rock potential for the strata at these locations is poor. In other areas where the thermal maturity is not as high, for example in Eagle Plain basin where Canol and Imperial formation strata is in the oil window (Link and Bustin, 1989; Lane *et al*., 2010), the source rock potential is more favourable.

Organic petrology revealed the presence of mainly amorphous kerogen with minor amounts of alginite derived vitrinite and bitumen macerals and negligible amounts of recycled or reworked terrestrial plant derived inertinite macerals and *Tasmanites* algae in the Road River Group and Canol Formation. In contrast, organic matter within the Imperial Formation is described as organically lean, containing minor vitrinite, inertinite and bitumen macerals. Kerogen type is fundamental to the determination of what ranges of hydrocarbon will be produced and affects adsorptive capacity (Faraj, 2009). The type of organic matter within the Road River Group and Canol Formation can be categorized as consisting of a mix of types I and II kerogen which are oil-prone. Alginite, such as *Tasmanites,* is frequently a major contributor to type I kerogen (Peters *et al*., 2005).

VR data indicates that there is a regional trend of decreasing thermal maturity southward along the flank of the Richardson Mountains. This is in part due to differential uplift on major structures that strike sub-parallel to the anticlinorium axis (*e.g.*, Lane, 1996; Lane *et al*. 2007); as well as to presumed deeper burial in the north. No obvious trend exists between the level of thermal maturity and the stratigraphic interval. In the south, where vitrinite reflectance values for the Canol are 1.89-1.97 %Ro_R, the level of thermal maturity is at the upper limit of the wet/dry gas generation zone. Moving north to the Rich and Fox properties, where vitrinite reflectance values for all formations is >2.0 %Ro_R, the strata are within the dry gas generation zone. It is believed that strata with vitrinite reflectance values greater than 4 %Ro are barren of hydrocarbons (North, 1985), however post-mature thermogenic shale-gas has been produced from the Marcellus Formation in the eastern Pennsylvania at Ro_R values >3.0 (*e.g.,* Laughrey *et al*., 2011). To the west of the Richardson anticlinorium, in Eagle Plain basin, the maturity of the Canol and Imperial formations in the subsurface decreases from the dry gas window to the oil window (Link and Bustin, 1989; Lane *et al*., 2010). This trend probably reflects greater depth of burial at the level of Devonian shale in the former Richardson trough. However, variations in the paleogeothermal gradient in the region cannot be ruled out (Link and Bustin, 1989). These results highlight the potential for source rock generation and shale gas/liquids in Eagle Plain basin.

Mineralogical composition is an important property in characterizing the mechanical properties of shale in order to design optimal techniques for natural gas extraction, *e.g.*, hydraulic fracturing. Hydraulic fracturing increases the amount of shale reservoir contacted by a wellbore by creating an artificial fracture network through fluid stimulation. Brittle shale is more likely to respond to this type of stimulation by creating a complex fracture network (Clarkson *et al*., 2011). According to Passey *et al*. (2010), current producing shale-gas reservoirs tend to have <50% clay, and the reservoirs that contain >50% quartz or carbonate are more brittle and respond well to current stimulation practises. Using these guidelines, XRD results indicate that all strata examined can be characterized as brittle, with high silica components enhanced by variable carbonate contents, and minor to negligible clay contents. The Canol Formation and Road River Group are comparatively brittle, with the Canol consistently highly siliceous with greater than 91% quartz and low (typically <3%) carbonate and clay components. Road River Group shale has a more varied lithology with 62 to 96% quartz and up to 37% carbonate minerals (mostly calcite) and up to 4% mica/illite (in core samples). Imperial Formation

shale is overall less brittle than the Canol Formation or Road River Group as the clay component is generally higher (up to 17% mica, illite, mixed-layer clay and/or clinochore), however, the considerable quartz content (82 to 90%) characterizes it as brittle regardless. Further assessment using a scanning electron microscope (SEM) may provide more accurate mineralogical information than standard XRD techniques, removing the possibility of quartz overestimation and clay underestimation mentioned previously. SEM also provides further information about the rock fabric and natural fracture patterns used to assess mechanical and flow properties of shale (Spencer *et al*., 2010). In addition, further information about the quartz component would enhance this study, as it has been suggested that the most effective quartz component for reservoir stimulation is biogenic opaline silica (Jarvie *et al*., 2007) and that detrital quartz is less effective (Thyberg *et al*., 2009).

All strata analysed herein have the potential to host unconventional hydrocarbons under proper burial conditions. The Canol Formation is the most promising unit as it is extremely brittle due to its high silica contents, mineralogically consistent throughout the study region, has very good to excellent total organic carbon contents and has favourable thermal maturity in Eagle Plain basin. The Road River Group also has favourable TOC and XRD values, however, previous studies from limited well data suggest it has poor source rock potential regionally in northern Yukon (Link and Bustin, 1989). Imperial Formation strata has lower TOC contents than the other units, but it is brittle and found to be favourably thermally mature in some Eagle Plain wells.

SUMMARY AND CONCLUSIONS

Fresh diamond drill core samples from Paleozoic shale of the Road River Group and Canol and Imperial formations in the Richardson Mountains immediately east of Eagle Plain basin were analysed for Rock-Eval pyrolysis, organic petrology, and vitrinite reflectance to assess organic matter quantity, quality, and thermal maturity. X-ray diffraction was conducted to assess quartz, clay, and carbonate mineralogy.

Results of this study suggest that the strata examined have the potential to host unconventional hydrocarbons in the region, under favourable burial conditions. Based on TOC values, Canol Formation and Road River Group contain the most organic-rich strata of that studied, and may have been more organic-rich in the past. At the current sample locations, however, the high thermal maturity of strata suggests they have limited generative potential. Based on organic petrology, it was determined that the organic matter consists of a mix of types I and II which coincide with oil-prone kerogen. Vitrinite reflectance illustrates the levels of thermal maturation for all strata are very high, ranging from 1.89 to 3.86 $\%Ro_R$, with 93% of samples >2.0 $\%Ro_R$ indicating most of the strata have matured beyond the oil and wet gas windows into the dry gas generation zone. The maturity data also demonstrate a general trend of decreasing thermal maturity from the Fox property in the north to the Pe property in the south for all geological units assessed. X-ray diffraction results indicate that all strata are dominantly siliceous, and thus candidates for successful hydraulic fracturing programs, however, the Canol Formation is the most mineralogically consistent with over 91% quartz in all samples. Road River Group strata are slightly more mineralogically variable than Canol Formations samples, with silica content ranging from 62-96% and carbonate content up to 37%. The Imperial Formation contains over 82% quartz with up to 17% clay.

Initial results from this diamond drillhole study were presented in Allen *et al*. (2011) which presented Rock-Eval, XRD mineralogy, and palynological determinations of Road River Group, and Canol and Imperial strata from Rich property core. This study includes core data from two additional locations (Fox and Pe) and surface field samples from the Rich property. The inclusion of data from locations both south and north of the Rich property in this paper expands the geographic extent of these analyses and illustrates improved understanding of thermal maturity trends along strike. In addition, this study includes vitrinite reflectance data and a summary description of the organic petrology. The organic petrology results provide insight into the types of organic matter present in the strata as determination through geochemical techniques was not possible due to the advanced thermal maturity of the organic matter.

It is important to mention that this study would not have been possible without data sharing between the minerals and oil and gas sectors, specifically the prompt provision of diamond drill core that may otherwise have been subjected to weathering in the field. Further collaboration between these sectors is encouraged in advancing the understanding of Yukon geology.

ACKNOWLEDGEMENTS

This project, including field logistics and all analytical support, was funded by the Earth Sciences Sector, Natural Resources Canada, Geo-Mapping for Energy and Minerals (GEM-Energy) initiative. This project was also funded in part by YGS and Northern Cross (Yukon) Limited (NCY). Fireweed helicopters Ltd. provided reliable and safe helicopter support. Special acknowledgement is extended to Archer Cathro & Associates (1981) Limited who donated core for this project. The manuscript was reviewed by Lee Pigage, Yukon Geological Survey, and Mark Obermajer, Geological Survey of Canada. The manuscript is ESS Contribution No. 20110357.

REFERENCES

Allen, T.L., 2010. Field notes on the Upper Devonian Imperial Formation (NTS map sheet 106L), Tetlit Creek, east Richardson Mountains, Yukon. *In:* Yukon Exploration and Geology 2009, K.E. MacFarlane, L.H. Weston and L.R. Blackburn (eds.), Yukon Geological Survey, p. 1-21.

Allen, T.L., Fraser, T.A., and Lane, L.S., 2011. Preliminary results from a diamond drill hole study to assess shale gas potential of Devonian strata, Eagle Plain, Yukon. *In:* Yukon Exploration and Geology 2010, K.E. MacFarlane, L.H. Weston and C. Relf (eds.), Yukon Geological Survey, p. 1-17.

Bassett, H.G., 1961. Devonian stratigraphy, central Mackenzie River region, Northwest Territories, Canada. *In:* Geology of the Arctic, G.O. Raasch (ed.), Alberta Society of Petroleum Geologists and University of Toronto Press, vol. 1, p. 481-498.

Braman, D.R. and Hills, L.V., 1992. Upper Devonian and Lower Carboniferous miospores, western District of Mackenzie and Yukon Territory, Canada. Palaeontolographica Canadiana, no. 8, 97 p.

Clarkson, C.R., Aguilera, R., Pederson, P.K., and Spencer, R.J., 2011. Shale Gas Part 6 – Influence of Technology on Shale Gas Development. CSPG Reservoir, vol. 38, no. 2, p. 23-29.

Daly, A.R. and J.D. Edman, 1987. Loss of organic carbon from source rocks during thermal maturation. American Association of Petroleum Geologists Bulletin, vol. 71, p. 546.

Dembicki, H. Jr., 2009. Three common source rock evaluation errors made by geologists during prospect or play appraisals. American Association Petroleum Geologists Bulletin, vol. 93, no. 3, p. 341-356.

Dolby, G., 2010. Palynological analysis of core, cuttings and outcrop samples from the GEM Yukon Basins Project. Dolby and Associates Report # 2010.9. Internal report prepared for Natural Resources Canada, Calgary, Alberta, 21 p.

Espitalié, J., Deroo, G., and Marquis, F., 1985. Rock Eval Pyrolysis and Its Applications. Preprint; Institut Française du Petrole, Geologie No. 27299, 72 p. English translation of, La pyrolyse Rock-Eval et ses applications, Premiere, Deuxieme et Troisieme Parties, in Revue de l'Institut Francais du Petrole, vol. 40, p. 563-579 and 755-784; vol. 41, p. 73-89.

Faraj, B. 2009. Shale gas critical fundamentals, techniques and tools for exploration analysis. Canadian Society of Petroleum Geologists Short Course # SC0902, October 26, 2009.

Fowler, M., Snowdon, L., and Stasiuk, V., 2005. Applying petroleum geochemistry to hydrocarbon exploration and exploitation. American Association of Petroleum Geologists Short Course Notes, June 18-19, 2005, Calgary, Alberta, 224 p.

Fraser, T. and Hogue, B., 2007. List of Wells and Formation Tops, Yukon Territory, version 1.0. Yukon Geological Survey, YGS Open File 2007-5, 1 p., plus spreadsheet.

Fritz, W.H., 1985. The basal contact of the Road River Group - a proposal for its location in the type area and in other selected areas in the northern Canadian Cordillera. *In:* Current Research, Part B, Geological Survey of Canada, Paper 85-1B, p. 205-215.

Gal, L.P., Allen, T.L., Hadlari, T., and Zantvoort, W.G., 2009. Chapter 10 – Petroleum Systems Elements. *In:* Regional Geoscience Studies and Petroleum Potential, Peel Plateau and Plain, Northwest Territories and Yukon: Project Volume, L.J. Pyle and A.L. Jones (eds.), Northwest Territories Geoscience Office and Yukon Geological Survey, NWT Open File 2009-02 and YGS Open File 2009-25, p. 477-549.

Gordey, S.P. and Makepeace, A.J., 1999. Yukon digital geology. Geological Survey of Canada, Open File D3826.

Goodfellow, W.D., 2011. Devonian shale-hosted Ni-Zn-Mo-PGE sulfide deposits, Yukon. *In:* Abstracts with Program, GAC/MAC 2011, May 25-27, Ottawa, p. 77.

Hadlari, T., Gal, L.P., Zantvoort, W.G., Tylosky, S.A., Allen, T.L., Fraser, T.A., Lemieux, Y., and Catuneanu, O., 2009. Chapter 7 – Upper Devonian to Carboniferous Strata I – Imperial Formation Play. *In:* Regional Geoscience Studies and Petroleum Potential, Peel Plateau and Plain, Northwest Territories and Yukon: Project Volume, L.J. Pyle and A.L. Jones (eds.), Northwest Territories Geoscience Office and Yukon Geological Survey, NWT Open File 2009-02 and YGS Open File 2009-25, p. 337-364.

Hall, K.W. and Cook, F.A., 1998. Geophysical transect of the Eagle Plains foldbelt and Richardson Mountains anticlinorium, northwestern Canada. Geological Society of America Bulletin, vol. 110, no. 3, p. 311-325.

Hamblin, A.P., 2006. The "Shale Gas" concept in Canada: a preliminary inventory of possibilities. Geological Survey of Canada Open File 5384, 103 p.

Héon, D., 2006. Mineral Assessment of the Eagle Plain Study Area, Yukon. Yukon Geological Survey, Open File 2006-3. Includes 2 reports: original study (103 p. plus 1 map) and update (12 p. plus 4 maps).

Hume, G.S. and Link, T.A., 1945. Canol investigations in the Mackenzie River area, Northwest Territories and Yukon. Geological Survey of Canada, Paper 45-16, 87 p.

Jacob, H., 1989. Classification, structure, genesis and practical importance of natural solid oil bitumen ("migra-bitumen"). International Journal of Coal Geology, vol. **11**, p. 65–79.

Jackson, D.E. and Lenz, A.C., 1962. Zonation of Ordovician and Silurian graptolites of northern Yukon, Canada. American Association of Petroleum Geologists Bulletin, vol. 46, p. 30-45.

Jarvie, D.M., Hill, R.J., Ruble, T.E., and Pollastro, R.M., 2007. Unconventional shale-gas systems: The Mississippian Barnett Shale of north-central Texas as one model for thermogenic shale-gas assessment. American Association of Petroleum Geologists Bulletin, vol. 91, no. 4, p. 475–499.

Lafargue, E., Espitalié, J., Marquis, F., and Pillot, D., 1998. Rock-Eval 6 applications in hydrocarbon exploration, production and soil contamination studies. Revue de l'Insitut Français du Petrole vol. 53, p. 421-437.

Lane, L.S., 1996. Geometry and tectonics of early Tertiary triangle zones, northeastern Eagle Plain, Yukon Territory. Bulletin of Canadian Petroleum Geology, vol. 44, p. 337-348.

Lane, L.S., 1998. Late Cretaceous-Tertiary tectonic evolution of northern Yukon and adjacent Arctic Alaska. American Association of Petroleum Geologists Bulletin, vol. 82, p. 1353-1371.

Lane, L.S., 2007. Devonian-Carboniferous paleogeography and orogenesis, northern Yukon and adjacent Arctic Alaska. Canadian Journal of Earth Sciences, vol. 44, p. 679-694.

Lane, L.S., 2010. Phanerozoic Structural Evolution of Eagle Plain, Yukon. Canadian Society of Petroleum Geologists, Reservoir, vol. 37, no.1, p. 11.

Lane, L. S. and Dietrich, J.R., 1995. Tertiary structural evolution of the Beaufort Sea - Mackenzie Delta region, Arctic Canada. Bulletin of Canadian Petroleum Geology, vol. 43, p. 293-314.

Lane, L.S., Utting, J., Allen, T.L., Fraser, T., and Zantvoort, W., 2007. Refinements to Lithostratigraphy, Biostratigraphy and Structural Geometry of the Devonian and Carboniferous Imperial and Tuttle Formations, eastern Eagle Plain, northern Yukon. CSPG-CSEG Annual Meeting, Calgary AB, Program and Abstracts Volume, p. 316-317; CD-ROM: 214S0131.

Lane, L.S., Snowdon, L.R., and Obermajer, M., 2010. Rock-Eval/TOC and oil show analyzer data for selected Yukon borehole samples. Geological Survey of Canada, Open File 6652, 1 CD-ROM.

Laughrey, C.D., Ruble, T.E., Lemmens, H., Kostelnik, J., Butcher, A.R., Walker, G., and Knowles, W., 2011. Black shale diagenesis: insights from integrated high-definition analyses of post-mature Marcellus Formation rocks, northeastern Pennsylvania. American Association of Petrology Geologists, Search and Discovery Article #110150.

Link, T.A., 1921. Unpublished geological report on the Fort Norman area: Imperial Oil Ltd., Calgary, Alberta, 81 p.

Link, C.M. and Bustin, R.M., 1989. Organic maturation and thermal history of Phanerozoic strata in northern Yukon and northwestern District of Mackenzie. Bulletin of Canadian Petroleum Geology, vol. 37, p. 266-292.

Link, C.M., Bustin, R.M., and Snowdon, L.R., 1989. Petroleum Source Potential and Depositional Setting of Phanerozoic Strata in northern Yukon and northwestern District of Mackenzie. Bulletin of Canadian Petroleum Geology, vol. 37, p. 293-315.

Mackowsky, M. –Th., 1982. Methods and tools of examination. *In:* Stach's Textbook of coal Petrology, 3rd ed., E. Stach, M.-Th. Mackowsky, M. Teichmüller, G.H. Taylor, D. Chandra, and R. Teichmüller (eds.), Berlin: Gerbruder Borntraeger, p. 295-299.

Mazzotti, W., Leonard, L.J., Hyndman, R.D., and Cassidy, J.F., 2008. Tectonics, Dynamics, and Seismic Hazard in the Canada-Alaska Cordillera. *In:* Active Tectonics and Seismic Potential of Alaska; American Geophysical Union, Geophysical Monograph Series, no. 179, p. 297-319.

Morrow, D.W., 1999. Lower Paleozoic Stratigraphy of Northern Yukon Territory and Northwestern District of Mackenzie. Geological Survey of Canada, Bulletin 538, 202 p.

Mukhopadyhay, P.K., 1994. Vitrinite reflectance as maturity parameter: petrographic and molecular characterization and its applications to basin modeling. *In*: Vitrinite reflectance as a maturity parameter, applications and limitations, P.K. Mukhopadyhay and W.G. Dow (eds.), American Chemical Society Symposium Series 570, p. 1-25.

Norris, A.W., 1985. Stratigraphy of Devonian outcrop belts in northern Yukon Territory and northwestern District of Mackenzie. Geological Survey of Canada, Paper 67-53, 287 p.

Norris, A.W., 1997. Devonian (Chapter 7). *In:* Geology and Mineral and Hydrocarbon Potential of Northern Yukon Territory and Northwestern District of Mackenzie, D.K. Norris (ed.), Geological Survey of Canada, Bulletin 422, p. 163-200.

Norris, D.K., 1984. Geology of the northern Yukon and northwestern District of Mackenzie. Geological Survey of Canada, Map 1581A.

North, F.K., 1985. Petroleum Geology, Allen & Unwin, London, 607 p.

Osadetz, K.G., Zhuoheng, C., and Bird, T.D., 2005. Petroleum Resource Assessment, Eagle Plain Basin and Environs, Yukon Territory, Canada. Yukon Geological Survey Open File 2005-2/Geological Survey of Canada, Open File 4922, 88 p.

Passey, Q.R., Bohacs, K.M., Esch, W.L., Klimentidis, R., and Sinha, S., 2010. From oil-prone source rock to gas-producing shale reservoir – geological and petrophysical characterization of unconventional shale-gas reservoirs. Society of Petroleum Engineers, CPS/SPE International Oil & Gas Conference and Exhibition, Beijing, China, 8-10 June, 2010, SPE 131350, 29 p.

Peters, K.E., 1986. Guidelines for evaluating petroleum source rock using programmed pyrolysis. American Association of Petroleum Geologists Bulletin, vol. 70, no. 3, p. 318-329.

Peters, K.E., Walters, C.C., and Moldowan, J.M., 2005. The Biomarker Guide, Volume 1. Biomarkers and Isotopes in the Environment and Human History. Cambridge University Press, New York, 471 p.

Pugh, D.C., 1983. Pre-Mesozoic geology in the subsurface of Peel River Map area, Yukon Territory and District of Mackenzie. Geological Survey of Canada, Memoir 401, 61 p.

Richards, B.C., Bamber, E.W., and Utting, J., 1997. Upper Devonian to Permian. *In:* Geology and Mineral and Hydrocarbon Potential of Northern Yukon Territory and Northwestern District of Mackenzie, D.K. Norris (ed.); Geological Survey of Canada, Bulletin 422, p. 201-251.

Snowdon, L.R., 1988. Petroleum source rock potential and thermal maturation reconnaissance in Eagle Plain, Yukon Territory. Geological Survey of Canada, Open File 1720, 115 p.

Spencer, R.J., Pedersen, P.K., Clarkson, C.R., and Aguilera, R., 2010. Shale Gas Part 3 – Shale Properties. CSPG Reservoir, vol. 37, no. 10, p. 26-29.

Tissot, B.P. and Welte, D.H., 1984. Petroleum Formation and Occurrence. Springer-Verlag, Berlin, Heidelberg, New York, Tokyo, 699 p.

Thyburg, B., Jahren, J., Winje, T., Bjorlykke, K., and Faleide, J.I., 2009. From mud to shale: rock stiffening by microquartz cementation. European Association of Geoscientists and Engineers, First Break, vol. 27, issue 2, p. 53-39.

Appendix A. *Summary of vitrinite reflectance data including sample descriptions. SD = standard deviation and N = number of measurements for corresponding average %Ro. Grey cells represent vitrinite equivalent values for measured pyrobitumen macerals based on Jacob (1989).*

Sample #	GSC Curation #	Downhole depth (m)	Unit	$\%Ro_R$	SD	N	Comments
FX07-02-6	C-491541	52.7	Canol	2.91	0.12	15	Overmature organic-rich black shale with major amount of interconnected network of sieve like amorphous kerogen with minor amount of alginite and alginite derived vitrinite and bitumen macerals, and rare amount of framboidal and tetrahedral pyrite minerals. Trace amount of Tasmanites, chitinozoans and inertinite macerals.
FX07-02-4	C-491539	64.0	Canol	3.00	0.14	22	Overmature organic-rich black shale with major amount of interconnected network of sieve like amorphous kerogen with minor amount of alginite and alginite derived vitrinite and bitumen macerals, and rare amount of framboidal and tetrahedral pyrite minerals. Trace amount of Tasmanites, chitinozoans and inertinite macerals.
FX07-02-3	C-491538	79.0	Road River	3.09	0.09	15	Overmature organic-rich black shale with major amount of interconnected network of sieve like amorphous kerogen with minor amount of alginite and alginite derived vitrinite and bitumen macerals, and rare amount of framboidal and tetrahedral pyrite minerals. Trace amount of Tasmanites, chitinozoans and inertinite macerals.
FX07-02-1	C-491536	106.9	Road River	3.11	0.09	22	Overmature organic-rich black shale with major amount of interconnected network of sieve like amorphous kerogen with minor amount of alginite and alginite derived vitrinite and bitumen macerals, and rare amount of framboidal and tetrahedral pyrite minerals. Trace amount of Tasmanites, chitinozoans and inertinite macerals.
FX07-03-9	C-491553	33.3	Canol	3.59	0.11	18	Overmature organic-rich black shale with major amount of interconnected network of sieve like amorphous kerogen with minor amount of alginite and alginite derived vitrinite and bitumen macerals, and rare amount of framboidal and tetrahedral pyrite minerals. Trace amount of Tasmanites, chitinozoans and inertinite macerals.
FX07-03-5	C-491549	87.5	Canol	3.13	0.09	21	Overmature organic-rich black shale with major amount of interconnected network of sieve like amorphous kerogen with minor amount of alginite and alginite derived vitrinite and bitumen macerals, and rare amount of framboidal and tetrahedral pyrite minerals. Trace amount of Tasmanites, chitinozoans and inertinite macerals.
FX07-03-3	C-491547	111.5	Road River	3.14	0.15	28	Overmature organic-rich black silty shale with major amount of interconnected network of sieve like amorphous kerogen with minor amount of alginite and alginite derived vitrinite and bitumen macerals, and rare amount of framboidal and tetrahedral pyrite minerals. Trace amount of Tasmanites, chitinozoans, radiolaria and inertinite macerals.

Appendix A continued.

Sample #	GSC curation #	Downhole depth (m)	Unit	$\%Ro_R$	SD	N	Comments
FX07-03-2	C-491546	128.6	Road River	3.86	0.14	28	Overmature organic-rich black silty shale with major amount of interconnected network of sieve like amorphous kerogen with minor amount of alginite and alginite derived vitrinite and bitumen macerals, and rare amount of framboidal and tetrahedral pyrite minerals. Trace amount of Tasmanites, chitinozoans, radiolaria and inertinite macerals.
FX07-03-1	C-491545	139.0	Road River	2.99	0.08	21	Overmature organic-rich black silty shale with major amount of interconnected network of sieve like amorphous kerogen with minor amount of alginite and alginite derived vitrinite and bitumen macerals, and rare amount of framboidal and tetrahedral pyrite minerals. Trace amount of Tasmanites, chitinozoans, radiolaria and inertinite macerals.
RI07-02-5	C-491565	44.7	Road River	2.21	0.13	4	Framboidal pyrite-rich black shale with trace amount of bitumen and migrabitumen macerals (associated with carbonate minerals in pores or in fractures) brecciated within micrinite-rich spent amorphinite kerogen. Rare amount of alginite derived vitrinite macerals and Tasmanites alginite and trace of amount of calcite filled radiolaria microfossils, chitinozoans and Tasmanites alginite.
RI07-02-1	C-491561	105.6	Road River	2.25	0.12	22	Carbonate-rich black shale with minor of amount of calcite filled radiolaria microfossils and Tasmanites alginite. Mainly small alginite derived amorphinite lenses and bitumen macerals.
RI07-07A-12	C-491526	37.8	Canol	2.07	0.11	22	Framboidal pyrite-rich black shale with trace amount of bitumen and migrabitumen macerals (mainly granular and associated with carbonate minerals in pores or in fractures) brecciated within micrinite-rich spent amorphinite kerogen. Rare amount of alginite derived vitrinite macerals and trace of amount of calcite filled radiolaria microfossils, chitinozoans and Tasmanites alginite.
RI07-07A-6	C-491520	91.0	Canol	2.28	0.15	19	The microstratigraphy shows two distinct matrices consisting of organic and pyrite rich black shale with mostly sieve like amorphinite kerogen and organic-rich mostly amrphinite kerogen, pyrite lean black shale matrix. Trace amount of alginite macerals possibly from prosinophyte.
RI07-07A-5	C-491519	102.3	Canol	2.30	0.10	9	Framboidal pyrite-rich black shale with trace amount of bitumen and migrabitumen macerals (mainly granular and associated with carbonate minerals in pores or in fractures) brecciated within micrinite-rich spent amorphinite kerogen. Rare amount of alginite derived vitrinite macerals and trace of amount of calcite filled radiolaria microfossils, chitinozoans and Tasmanites alginite.

Appendix A continued.

Sample #	GSC curation #	Downhole depth (m)	Unit	%Ro_R	SD	N	Comments
RI07-07A-2	C-491516	140.2	Canol	2.48	0.11	17	Black shale with mostly sieve like amorphous amorphinite kerogen lenses and rare amount of alginite derived vitrinite and bitumen (mostly granular pore filling migrabitumen) macerals. Trace amount of chitinozoans and fracture filling dolomite mineral.
RI07-07A-1	C-491515	166.5	Road River	2.77	0.09	17	Black shale containing minor amount of framboidal pyrite with mostly amorphous amorphinite kerogen and rare amount of alginite derived vitrinite and bitumen macerals. Trace amount of Tasmanites alginite and chitinozoans were also observed together mostly small prosinophyte alginite.
RI07-16-5	C-491558	58.5	Canol	2.27	0.09	12	Framboidal pyrite-rich black shale with trace amount of bitumen and migrabitumen macerals (associated with carbonate minerals in pores or in fractures) within amorphinite-rich matrix. Rare amount of alginite derived vitrinite macerals and Tasmanites alginite.
RI07-16-3	C-491556	86.0	Canol	2.43	0.07	19	black shale with evidence of dolomitizing fluid intrusion. Mainly spent amorphinite kerogen with rare bitumen maceral and trace amount of alginite (possibly prasinophyte) derived vitrinite macerals and chitinozoans. Trace amount of bitumen macerals showing very fine grain and minor anisotropic morphology, and high pyrite inclusion indication of high sulphides.
RI07-16-2	C-491555	103.1	Road River	2.56	0.12	18	Black shale with evidence of dolomitizing fluid intrusion. Mainly spent amorphinite kerogen with rare bitumen maceral and trace amount of alginite (possibly prasinophyte) derived vitrinite macerals and chitinozoans. Rare amount of bitumen macerals proximal to the dolomite matrix shows granular and minor anisotropic morphology, and high pyrite inclusion indication of high sulphides.
RI07-16-1	C-491554	121.9	Road River	2.43	0.06	10	Black shale with evidence of dolomitizing fluid intrusion. Mainly spent amorphinite kerogen with rare bitumen maceral and trace amount of alginite (possibly prasinophyte and Tasmanites) derived vitrinite macerals. Some bitumen macerals proximal to the dolomite matrix shows granular and minor anisotropic morphology, and high pyrite inclusion indication of high sulphides.
RI07-20-5	C-491571	119.3	Canol	2.33	0.09	18	Framboidal pyrite-rich black shale with trace amount of bitumen and migrabitumen macerals (associated with carbonate minerals in pores or in fractures) brecciated within micrinite-rich spent amorphinite kerogen matrix. Rare amount of alginite derived vitrinite macerals, trace of amount of calcite filled radiolaria microfossils, chitinozoans and possibly Leiophaeridia alginite.

Appendix A continued.

Sample #	GSC curation #	Downhole depth (m)	Unit	%Ro_R	SD	N	Comments
RI07-20-1	C-491567	185.9	Canol?	2.51	0.13	15	Black shale with mainly spent amorphinite kerogen with minor amount small lenses of bitumen macerals and framboidal pyrite, and trace amount of alginite (possibly prasinophyte) derived vitrinite macerals. Trace amount of chitinozoans. Rare amount of bitumen macerals proximal to the dolomite matrix shows granular and minor anisotropic morphology, and high pyrite inclusion indication of high sulphides.
R108-24-45	C-486512	66.9	Imperial	2.33	0.22	6	Siltstone with minor amount amount organic and pyrite (framboidal and euhedral crystal). Presence of phosphatic nodules, inertinite. Rare isotropic vitrinite and bitumen lenses.
R108-24-41	C-486508	129.6	Imperial	3.00	0.13	17	Organic and pyrite (framboidal and euhedral crystal) rich silty shale. Presence of phosphatic nodules, inertinite. Rare isotropic vitrinite and bitumen lenses.
R108-24-37	C-486504	184.5	Imperial	2.68	0.08	2	Organic and pyrite (framboidal and euhedral crystal) rich silty shale. Presence of phosphatic nodules, inertinite. Rare isotropic vitrinite and bitumen lenses.
R108-24-30	C-486497	244.1	Imperial	3.11	0.19	12	Organic and pyrite (framboidal and euhedral crystal) rich silty shale. Presence of phosphatic nodules, inertinite. Rare isotropic vitrinite and bitumen lenses.
R108-24-26	C-486493	302.8	Imperial	2.89	0.18	38	Organic and pyrite (framboidal and euhedral crystal) rich silty shale. Presence of phosphatic nodules, inertinite. Rare isotropic vitrinite and bitumen lenses.
R108-24-21	C-486488	360.0	Imperial	3.09	0.14	8	Mainly limestone with minor amount of partially dolomitized siltstone containing minor dark amorphous styloccumulates kerogen and rare high reflecting isotropic pyrobitumen.
R108-24-20	C-486487	366.8	Imperial	2.90	0.13	14	Organic and pyrite (framboidal and euhedral crystal) rich silty shale. Presence of phosphatic nodules, inertinite. Rare anisotropic vitrinite and bitumen lenses evidence of thermal cracking.
R108-24-19	C-486486	376.2	Canol	2.90	0.16	20	Pyrite (mainly framboidal) rich shale. Mainly primary bitumen derived from the thin interconnected amorphinite lenses. Silicified radiolaria and corbonate filled forams and alginite, inertinite and phosphatic nodules were also observed.
R108-24-18	C-486485	384.3	Canol	2.89	0.23	14	similar to above sample
R108-24-16	C-486483	401.7	Canol	2.77	0.28	30	Pyrite (mainly framboidal) rich shale with mainly brown amorphous kerogen with small particle (lenses), rare pyrobitumen maceral observed between carbonates grains.
R108-24-14	C-486481	425.0	Canol	2.83	0.20	20	Pyrite (mainly framboidal) rich shale. Mainly primary bitumen derived from the thin interconnected amorphinite lenses. Silicified radiolaria and corbonate filled forams and alginite, inertinite and phosphatic nodules were also observed.
R108-24-8	C-486474	494.5	Canol	2.76	0.23	15	Pyrite (mainly framboidal and sulphide-rich organic coaly lenses) rich shale. Mainly primary bitumen derived from the thin interconnected amorphinite lenses.

Appendix A continued.

Sample #	GSC curation #	Downhole depth (m)	Unit	%Ro_R	SD	N	Comments
R108-24-1	C-486467	565.0	Canol	2.88	0.28	7	Amorphinite and pyrite (mainly framboidal) rich shale with rare vitrinite and pyrobitumen lenses. Thin interconnected amorphinite macerals.
RI08-25-22	C-491595	49.5	Imperial	2.09	0.07	3	Organically lean matrix minor amount of vitrinite and bitumen maceral brecciated between fine grain siltstone matrix. Some sporinite and semifusinite derived inertinite macerals are of the sample thermal maturity as the bitumen and vitrinite macerals.
RI08-25-18	C-491591	105.5	Imperial	2.08	0.16	3	Organically lean matrix minor amount of vitrinite and bitumen maceral brecciated between fine grain siltstone matrix. Some sporinite and semifusinite derived inertinite macerals are of the sample thermal maturity as the bitumen and vitrinite macerals.
RI08-25-14	C-491587	163.8	Imperial	2.25	0.03	4	Organically lean matrix minor amount of vitrinite and bitumen maceral brecciated between fine grain siltstone matrix. Some sporinite and semifusinite derived inertinite macerals are of the sample thermal maturity as the bitumen and vitrinite macerals.
RI08-25-10	C-491583	225.1	Imperial	2.41	0.03	7	Organically lean matrix minor amount of vitrinite and bitumen maceral brecciated between fine grain siltstone matrix. Some inertinite macerals are of the sample thermal maturity as the bitumen and vitrinite macerals.
RI08-25-5	C-491578	286.5	Imperial	2.32	0.04	4	Organically lean matrix minor amount of vitrinite and bitumen maceral brecciated between fine grain siltstone matrix. Some inertinite macerals are of the sample thermal maturity as the bitumen and vitrinite macerals.
RI08-25-1	C-491574	343.5	Imperial	2.47	0.09	3	Organically lean matrix minor amount of vitrinite and bitumen maceral brecciated between fine grain siltstone matrix. Some inertinite macerals are of the sample thermal maturity as the bitumen and vitrinite macerals.
PE07-07-6	C-491532	99.4	Canol	1.89	0.09	21	Framboidal pyrite-rich dominated black shale matrix with trace amount of bitumen and migrabitumen macerals (mainly granular and associated with carbonate minerals in pores or in fractures) brecciated within micrinite-rich spent amorphinite kerogen. Trace amount of alginite derived vitrinite macerals and terrestrial plant derived inertinite macerals.
PE07-07-5	C-491531	109.7	Canol	1.97	0.09	14	Framboidal pyrite-rich black shale with trace amount of bitumen and migrabitumen macerals (mainly granular and associated with carbonate minerals in pores or in fractures) brecciated within micrinite-rich spent amorphinite kerogen. Trace amount of alginite derived vitrinite macerals and terrestrial plant derived inertinite macerals.
PE07-07-1	C-491527	164.2	Canol	1.89	0.13	10	Framboidal pyrite-rich black shale with trace amount of bitumen and migrabitumen macerals (mainly granular and associated with carbonate minerals in pores or in fractures) brecciated within micrinite-rich spent amorphinite kerogen. Trace amount of alginite derived vitrinite macerals and terrestrial plant derived inertinite macerals.

Appendix B. *Mineral composition raw data based on XRD semi-quantitative analysis (expressed in mineral ratio percent) of black shale core samples and surface field samples. Highlighted samples refer to carbonate-rich shale (R108-24-21) and a siderite nodule (R108-24-25).* = mixed-layer clay; ** = surface field samples; and + = chlorite and/or kaolinite.*

Sample #	GSC curation #	Downhole depth (m)	Fm	M.L.C.*	Mica/ Illite	Clino-chlore	Gyp	Qtz	Fldspr	Cal	Dol	Sd	Py	Others	Qtz	Total Carb	Total Clay	Sum Qtz, Carb & Clay	% Qtz	% Carb	% Clay
RI08-25-22	C491595	49.5	Imperial	2.0	3.0	9.0		82.0	2.0(Na)				2.0		82.0	0.0	14.0	96.0	85.4	0.0	14.6
RI08-25-20	C491593	77.5	Imperial	2.0	3.0	6.0		81.0	tr			6.0	2.0	Siderite-6%	81.0	6.0	11.0	98.0	82.7	6.1	11.2
RI08-25-18	C491591	105.5	Imperial	2.0	3.0	5.0		85.0	3.0(Na)				2.0		85.0	0.0	10.0	95.0	89.5	0.0	10.5
RI08-25-16	C491589	134.5	Imperial	2.0	3.0	5.0		87.0					3.0		87.0	0.0	10.0	97.0	89.7	0.0	10.3
RI08-25-14	C491587	163.8	Imperial	2.0	3.0	7.0		82.0	2.0(Na)		2.0		2.0	Fe dolomite	82.0	2.0	12.0	96.0	85.4	2.1	12.5
RI08-25-12	C491585	194.4	Imperial	3.0	3.0	3.0		84.0			2.0		5.0	Fe dolomite	84.0	2.0	9.0	95.0	88.4	2.1	9.5
RI08-25-10	C491583	225.1	Imperial	2.0	3.0	6.0		86.0					3.0		86.0	0.0	11.0	97.0	88.7	0.0	11.3
RI08-25-8	C491581	255.7	Imperial	3.0	4.0	7.0		84.0	tr				2.0		84.0	0.0	14.0	98.0	85.7	0.0	14.3
RI08-25-5	C491578	286.5	Imperial	3.0	4.0	6.0		85.0	tr				2.0		85.0	0.0	13.0	98.0	86.7	0.0	13.3
RI08-25-3	C491576	314.7	Imperial	3.0	3.0	7.0		83.0	2.0(Na)				2.0		83.0	0.0	13.0	96.0	86.5	0.0	13.5
RI08-25-1	C491574	343.5	Imperial	3.0	4.0	6.0		85.0					2.0		85.0	0.0	13.0	98.0	86.7	0.0	13.3
RI08-24-47	C491514	39.3	Imperial	2.0	3.0	5.0	tr	84.0	4.0(Na)				2.0		84.0	0.0	10.0	94.0	89.4	0.0	10.6
RI08-24-45	C491512	66.9	Imperial	2.0	3.0	6.0		84.0	3.0(Na)		1.0		1.0		84.0	1.0	11.0	96.0	87.5	1.0	11.5
RI08-24-43	C491510	96.3	Imperial	2.0	2.0	5.0		85.0	2.0(Na)		2.0		2.0		85.0	2.0	9.0	96.0	88.5	2.1	9.4
RI08-24-41	C491508	129.6	Imperial	3.0	4.0	8.0		82.0					3.0		82.0	0.0	15.0	97.0	84.5	0.0	15.5
RI08-24-39	C491506	155.0	Imperial	3.0	4.0	5.0		86.0					2.0		86.0	0.0	12.0	98.0	87.8	0.0	12.2
RI08-24-37	C491504	184.5	Imperial	3.0	4.0	10.0		81.0					2.0		81.0	0.0	17.0	98.0	82.7	0.0	17.3
RI08-24-34	C491501	214.3	Imperial	3.0	4.0	4.0		87.0					2.0		87.0	0.0	11.0	98.0	88.8	0.0	11.2
RI08-24-30	C486497	244.1	Imperial	3.0	4.0	7.0		84.0					2.0		84.0	0.0	14.0	98.0	85.7	0.0	14.3
RI08-24-28	C486495	273.2	Imperial	3.0	5.0	7.0		83.0					2.0		83.0	0.0	15.0	98.0	84.7	0.0	15.3
RI08-24-26	C486493	302.8	Imperial	3.0	4.0	4.0		85.0				2.0	2.0	Siderite-2%	85.0	2.0	11.0	98.0	86.7	2.0	11.2
RI08-24-25	C486492	315.2	Imperial	2.0	2.0	5.0		36.0				55.0		Siderite-55%	36.0	55.0	9.0	100.0	36.0	55.0	9.0
RI08-24-23	C486490	330.9	Imperial	3.0	3.0	2.0		81.0	2.0(Na)		4.0	3.0	2.0	Siderite-3%	81.0	7.0	8.0	96.0	84.4	7.3	8.3
RI08-24-21	C486488	360.0	Imperial		2.0			45.0		2.0	36.0		15.0		45.0	38.0	2.0	85.0	52.9	44.7	2.4
RI08-24-20	C486487	366.8	Imperial?	tr	5.0			88.0	tr				7.0		88.0	0.0	5.0	93.0	94.6	0.0	5.4
FX07-02-8	C491543	25.8	Canol		2.0		41.0	53.0	1.0(K), 2.0(Na)					Anhydrite?-1%	53.0	0.0	2.0	55.0	96.4	0.0	3.6
FX07-02-6	C491541	52.7	Canol		1.0		5.0	90.0	3.0(K), 1.0(Na)						90.0	0.0	1.0	91.0	98.9	0.0	1.1

Fm = Formation *Qtz = Quartz* *Cal = Calcite* *Sd = Siderite* *Carb = Carbonate*

Gyp = Gypsum *Fldspr = Feldspars* *Dol = Dolomite* *Py = Pyrite*

Appendix B continued

Sample	GSC curation #	Downhole depth (m)	Fm	M.L.C.*	Mica/ Illite	Clino-clore	Gyp	Qtz	Fldspr	Cal	Dol	Sd	Py	Others	Qtx	Total Carb	Total Clay	Sum Qtz, Carb & Clay	% Qtz	% Carb	% Clay
FX07-02-4	C491539	64.0	Canol		1.0		4.0	92.0	2.0(K)					Augite-1%	92.0	0.0	1.0	93.0	98.9	0.0	1.1
FX07-03-9	C491553	33.3	Canol		1.0		2.0	93.0	1.0(k)	3.0					93.0	3.0	1.0	97.0	95.9	3.1	1.0
FX07-03-7	C491551	60.7	Canol		4.0		tr	85.0	3.0(K)	2.0	1.0		3.0	Sphalerite?-2%	85.0	3.0	4.0	92.0	92.4	3.3	4.3
FX07-03-5	C491549	87.5	Canol		1.0			89.0	1.0(K)	7.0			1.0	Sphalerite?-1%	89.0	7.0	1.0	97.0	91.8	7.2	1.0
RI07-07A-12	C491526	37.8	Canol		1.0		1.0	90.0					8.0		90.0	0.0	1.0	91.0	98.9	0.0	1.1
RI07-07A-10	C491524	63.2	Canol		2.0		2.0	88.0					8.0		88.0	0.0	2.0	90.0	97.8	0.0	2.2
RI07-07A-6	C491520	91.0	Canol		1.0		tr	96.0		tr	1.0		2.0		96.0	1.0	1.0	98.0	98.0	1.0	1.0
RI07-07A-5	C491519	102.3	Canol	tr	1.0			94.0					5.0		94.0	0.0	1.0	95.0	98.9	0.0	1.1
RI07-07A-4	C491518	114.8	Canol		2.0			95.0					3.0		95.0	0.0	2.0	97.0	97.9	0.0	2.1
RI07-07A-2	C491516	140.2	Canol		1.0			96.0	1.0(K)	1.0			1.0		96.0	1.0	1.0	98.0	98.0	1.0	1.0
RI07-16-7	C491560	25.5	Canol		2.0			95.0	tr				3.0		95.0	0.0	2.0	97.0	97.9	0.0	2.1
RI07-16-5	C491558	58.5	Canol		2.0			92.0	2.0(K)				4.0		92.0	0.0	2.0	94.0	97.9	0.0	2.1
RI07-16-3	C491556	86.0	Canol		1.0			98.0	tr				1.0		98.0	0.0	1.0	99.0	99.0	0.0	1.0
RI07-20-7	C491573	85.9	Canol		1.0		1.0	95.0					3.0		95.0	0.0	1.0	96.0	99.0	0.0	1.0
RI07-20-5	C491571	119.3	Canol		1.0		tr	98.0					1.0		98.0	0.0	1.0	99.0	99.0	0.0	1.0
RI07-20-3	C491569	152.6	Canol		1.0			96.0				1.0	2.0	Siderite?-1%	96.0	1.0	1.0	98.0	98.0	1.0	1.0
RI07-20-1	C491567	185.9	Canol?		2.0			96.0					2.0		96.0	0.0	2.0	98.0	98.0	0.0	2.0
RI08-24-19	C486486	376.2	Canol		1.0			95.0			2.0		2.0		95.0	2.0	1.0	98.0	96.9	2.0	1.0
RI08-24-18	C486485	384.3	Canol		2.0		tr	95.0					3.0	Hercynite?-tr	95.0	0.0	2.0	97.0	97.9	0.0	2.1
RI08-24-17	C486484	393.0	Canol		2.0			96.0					2.0		96.0	0.0	2.0	98.0	98.0	0.0	2.0
RI08-24-16	C486483	401.7	Canol		2.0			91.0					6.0	Anhydrite-1%	91.0	0.0	2.0	93.0	97.8	0.0	2.2
RI08-24-14	C486481	425.0	Canol		1.0			93.0					5.0	Gahnite(ferroan)?-1%	93.0	0.0	1.0	94.0	98.9	0.0	1.1
RI08-24-12	C486479	458.8	Canol		tr			95.0					4.0	Hercynite?-1%	95.0	0.0	0.0	95.0	100.0	0.0	0.0
RI08-24-8	C486474	494.5	Canol		1.0			95.0					4.0		95.0	0.0	1.0	96.0	99.0	0.0	1.0
RI08-24-7	C486473	507.7	Canol		1.0			93.0					6.0		93.0	0.0	1.0	94.0	98.9	0.0	1.1

Fm = Formation *Qtz = Quartz* *Cal = Calcite* *Sd = Siderite* *Carb = Carbonate*

Gyp = Gypsum *Fldspr = Feldspars* *Dol = Dolomite* *Py = Pyrite*

Appendix B continued

Sample	GSC curation #	Downhole depth (m)	Fm	M.L.C.*	Mica/ Illite	Clino-clore	Gyp	Qtz	Fldspr	Cal	Dol	Sd	Py	Others	Qtx	Total Carb	Total Clay	Sum Qtz, Carb & Clay	% Qtz	% Carb	% Clay
RI08-24-4	C486470	531.3	Canol		1.0			93.0					5.0	Rutile?-1%	93.0	0.0	1.0	94.0	98.9	0.0	1.1
RI08-24-1	C486467	565.0	Canol		tr			99.0					1.0		99.0	0.0	0.0	99.0	100.0	0.0	0.0
10TLA-RICH-09M**	C542085		Canol	trace	1	tr+		99							99	0.0	1.0	100.0	99.0	0.0	1.0
PE07-07-8	C491534	82.5	Canol		1.0		1.0	92.0			3.0		2.0	Kaolinite-1%	92.0	3.0	1.0	96.0	95.8	3.1	1.0
PE07-07-5	C491531	109.7	Canol	1.0	1.0			96.0					2.0		96.0	0.0	2.0	98.0	98.0	0.0	2.0
PE07-07-3	C491529	137.2	Canol		2.0			89.0					5.0	Fluorapatite-4%	89.0	0.0	2.0	91.0	97.8	0.0	2.2
PE07-07-1	C491527	164.2	Canol		2.0		tr	94.0	tr				4.0		94.0	0.0	2.0	96.0	97.9	0.0	2.1
FX07-02-3	C491538	79.0	RR		3.0			88.0	2(K)	1.0			4.0	Sphalerite?-2%, Augite-tr	88.0	1.0	3.0	92.0	95.7	1.1	3.3
FX07-02-1	C491536	106.7	RR		4.0		tr	89.0	2(K)	2.0			3.0		89.0	2.0	4.0	95.0	93.7	2.1	4.2
FX07-03-3	C491547	111.5	RR		3.0			80.0	3.0(K)	4.0	8.0		2.0		80.0	12.0	3.0	95.0	84.2	12.6	3.2
FX07-03-2	C491546	128.6	RR		2.0			71.0	2(K)	13.0	11.0		1.0		71.0	24.0	2.0	97.0	73.2	24.7	2.1
FX07-03-1	C491545	139.0	RR		1.0			84.0	1(K)	11.0	2.0		1.0		84.0	13.0	1.0	98.0	85.7	13.3	1.0
RI07-07A-1	C491515	166.5	RR		2.0			92.0		4.0			2.0		92.0	4.0	2.0	98.0	93.9	4.1	2.0
RI07-16-2	C491555	103.1	RR		1.0			61.0		34.0	2.0		2.0		61.0	36.0	1.0	98.0	62.2	36.7	1.0
RI07-16-1	C491554	121.9	RR		1.0			88.0		10.0			1.0		88.0	10.0	1.0	99.0	88.9	10.1	1.0
RI07-02-5	C491565	44.7	RR		3.0		3.0	81.0		11.0			2.0		81.0	11.0	3.0	95.0	85.3	11.6	3.2
RI07-02-3	C491563	75.8	RR		2.0			75.0		19.0	1.0		3.0		75.0	20.0	2.0	97.0	77.3	20.6	2.1
RI07-02-1	C491561	105.6	RR		1.0			81.0	1.0	14.0			1.0	Sphalerite?-2	81.0	14.0	1.0	96.0	84.4	14.6	1.0
10TLA-RICH-09I**	C542083		RR		5	tr+		93	2 (Na)						93	0.0	5.0	98.0	94.9	0.0	5.1
10TLA-RICH-09K**	C542084		RR		6			91	tr (K)					Gypsum-1%, Pyrite-2%	91	0.0	6.0	97.0	93.8	0.0	6.2

Fm = Formation *Qtz = Quartz* *Cal = Calcite* *Sd = Siderite* *Carb = Carbonate*

Gyp = Gypsum *Fldspr = Feldspars* *Dol = Dolomite* *Py = Pyrite*